*horticulturae*

MDPI

*Article*

# Effects of Foliar Application of Calcium, Magnesium, and Boron on Leaf Nutritional and Physiological Traits and Fruit Yield of Korla Fragrant Pear

**Pengxue Jia [1,2], Yixin Ke [1,2], Xintong Gao [1,2], Enduo Liu [1,2], Kailong Wang [1,2] and Zhongping Chai [1,2,*]**

[1] College of Resources and Environment, Xinjiang Agricultural University, Urumqi 830052, China; jiapengxue663232@163.com (P.J.); 18963814232@163.com (Y.K.); gaogao13472367545@outlook.com (X.G.); led1826855938@163.com (E.L.); kl724169786@163.com (K.W.)

[2] Xinjiang Key Laboratory of Soil and Plant Ecological Processes, Xinjiang Agricultural University, Urumqi 830052, China

* Correspondence: czp@xjau.edu.cn; Tel./Fax: +86-991-876-3654

## Highlights

- Ca-Mg-B optimized leaf mineral nutrition and promoted leaf growth and physiological activity.
- Moderate Ca-Mg-B application improved photosynthesis-related traits, enhanced antioxidant defense capacity, and reduced oxidative damage.
- Responses of leaf traits and mineral accumulation were concentration-dependent.

## Abstract

Eight- to nine-year-old Korla fragrant pear (*Pyrus sinkiangensis* Yü) trees were used to evaluate the dose effects of a combined Ca–Mg–B foliar formulation on leaf nutritional and physiological traits and yield. A distilled-water control (CK) and three foliar spray treatments were established: L-CaMgB (0.1% Ca + 0.3% Mg + 0.15% B), M-CaMgB (0.2% Ca + 0.4% Mg + 0.25% B), and H-CaMgB (0.3% Ca + 0.5% Mg + 0.35% B). Foliar application increased leaf concentrations of N, P, Ca, Mg, Mn, Cu, Zn, and B, as well as SPAD values, leaf area index (LAI), single fruit weight, and yield, to varying degrees; these variables showed an increasing-then-decreasing trend with increasing concentration, with M-CaMgB performing best. Under M-CaMgB, leaf N, P, K, Ca, Mg, Mn, Cu, Zn, and B concentrations increased significantly by 59.09%, 21.04%, 49.38%, 51.41%, 40.27%, 73.53%, 53.29%, 26.35%, and 160.73%, respectively; SPAD and LAI increased significantly by 20.01% and 47.88%; Rubisco, SOD, CAT, and PAL activities were significantly enhanced by 171.41%, 127.26%, 128.90%, and 79.31%; and yield increased significantly by 33.78%. Correlation analysis revealed that Rubisco activity was highly significantly and positively correlated with N, P, Ca, and B ($p < 0.01$); yield showed the strongest correlations with LAI, PAL, CAT, and Rubisco, was highly significantly and positively correlated with N, P, K, Ca, Cu, Zn, and B ($p < 0.01$), and was significantly and positively correlated with Mn ($p < 0.05$). Mantel tests indicated that the association between mineral nutrients and leaf physiological traits was the strongest ($r = 0.85$, $p < 0.001$), followed by those between physiological traits and yield traits ($r = 0.75$, $p < 0.001$) and between mineral nutrients and yield traits ($r = 0.68$, $p < 0.001$). These exploratory results indicate strong associations among mineral nutrient accumulation, leaf physiological traits, and yield formation, suggesting that improved mineral nutrient status under the suitable Ca–Mg–B treatment may accompany enhanced leaf physiological performance and yield, whereas this coordinated association weakened at the higher application level. Based on these preliminary results, foliar co-application of

Check for updates

Academic Editors: Maria Roulia and Eloy Navarro-León

Received: 18 September 2026
Revised: 23 October 2026
Accepted: 26 October 2026
Published: 28 October 2026

**Copyright:** © 2026 by the authors. Licensee MDPI, Basel, Switzerland. This article is an open access article distributed under the terms and conditions of the Creative Commons Attribution (CC BY) license.

0.2% Ca fertilizer, 0.4% Mg fertilizer, and 0.25% B fertilizer is recommended for 8–9-year-old Korla fragrant pear trees, as it effectively improved leaf nutritional and physiological traits and achieved gains in both efficiency and yield.

**Keywords:** Korla fragrant pear; calcium; magnesium and boron; foliar application; leaf growth characteristics; yield

## 1. Introduction

Mineral nutrition represents a fundamental basis for the growth, development, productivity, and quality formation of fruit trees. Marschner [1] systematically elucidated the physiological and ecological functions of mineral nutrients in higher plants, providing a theoretical foundation for understanding the roles of essential mineral elements in horticultural crops. However, fertilizer management practices in many fruit production systems have long exhibited a structural imbalance, with excessive emphasis placed on the application of macronutrients, particularly nitrogen (N), phosphorus (P), and potassium (K), while the supply of medium- and micronutrients has often been neglected. Increasing evidence indicates that medium- and micronutrients, serving as essential structural components, enzyme activators, or cofactors of numerous metabolic pathways, play indispensable regulatory roles in plant growth, development, metabolism, and stress adaptation, thereby exerting profound effects on fruit yield and quality formation [2,3]. Calcium (Ca), magnesium (Mg), and boron (B) are essential medium- and micronutrients required for fruit tree growth and development, and they exert distinct yet complementary functions in plant structural formation, physiological metabolism, and reproductive development. The fruit enlargement stage represents a critical period for yield formation and quality development, during which rapid cell division, cell expansion, and substantial carbohydrate accumulation occur, resulting in increased demands for mineral nutrient availability. Calcium ions ($Ca^{2+}$), as important structural components of the cell wall, enhance cell wall mechanical strength and stability by cross-linking with galacturonic acid residues of pectic polysaccharides to form stable "egg-box" structures [4]. However, due to the limited phloem mobility of Ca within plants, root fertilization alone is often insufficient to meet the rapid Ca requirements during fruit enlargement. Therefore, foliar application provides an effective and rapid approach for improving Ca nutritional status in fruit trees. In addition to calcium, magnesium serves as the central atom of chlorophyll molecules and functions as an essential activator of ribulose-1,5-bisphosphate carboxylase/oxygenase (Rubisco), thereby directly regulating photosynthetic carbon assimilation. Appropriate magnesium supplementation can significantly increase leaf chlorophyll content and net photosynthetic rate, enhance photosynthetic efficiency, and promote the translocation of $^{13}C$-labeled photoassimilates to developing fruits, ultimately facilitating soluble sugar accumulation [5]. Furthermore, boron is primarily absorbed by plants in the form of boric acid ($H_3BO_3$) and contributes to cell wall stabilization through the formation of borate diester bonds with rhamnogalacturonan II (RG-II) in pectic networks [6,7]. During rapid fruit enlargement, increased requirements for cell division and cell wall remodeling necessitate adequate B availability. Appropriate B supply promotes cell wall formation and improves tissue extensibility, thereby providing structural support for fruit expansion and volume development [8]. Similarly, B plays an important role in maintaining normal leaf physiological functions and promoting photosynthetic product accumulation. As the primary organ responsible for carbon assimilation in fruit trees, leaf photosynthetic capacity directly determines the availability of carbon resources required for fruit development during the enlargement stage. Previous studies have shown that foliar B application increases the concentrations of N, P, K, B, and Zn in citrus leaves, improves

leaf nutritional status, and promotes vegetative growth and fruit development [9]. In recent years, combined fertilization strategies involving the co-application of secondary and micronutrients have attracted increasing attention; accumulating evidence indicates that calcium, magnesium, and boron are closely functionally interrelated at the levels of cell wall structure and carbon metabolism. Calcium and boron form complementary cross-linking networks in pectin matrices through ionic Ca–homogalacturonan (Ca-HG) interactions and covalent B–RG-II bonds, respectively, thereby jointly maintaining cell wall stability. Calcium also facilitates RG-II dimer formation, whereas boron-mediated cross-linking provides a structural framework for Ca-induced egg-box organization [8]. Studies in pummelo have demonstrated that combined foliar application of calcium and boron synergistically inhibits cell wall-degrading enzyme activities, reduces fruit cracking incidence, and enhances soluble sugar and vitamin C contents [10]. Magnesium, by improving photosynthetic efficiency, provides sufficient carbon resources for fruit development and works synergistically with Ca and B to enhance the allocation and accumulation of photosynthetic assimilates in fruits [5]. Research on Asian pear has shown that Ca-B foliar application within an appropriate concentration range exhibits good plant tolerance and effectively improves postharvest fruit quality, providing important evidence for Ca-B nutritional regulation in pear production [11]. In Valencia orange, previous studies evaluated foliar Ca application using calcium chloride combined with seaweed extract and boric acid, demonstrating that appropriate Ca supplementation effectively improved fruit yield performance and physicochemical characteristics [12]. Moreover, as the central component of chlorophyll molecules, Mg exhibits close nutritional interactions with other cations, particularly Ca. Maintaining an appropriate Ca-Mg balance is essential for stabilizing plant cellular structures, promoting photosynthesis, and improving crop productivity [13]. Leaves serve as the primary sites of photosynthesis and carbon assimilation in plants and therefore represent a critical physiological link between mineral nutrient regulation and fruit yield formation. Consequently, the synergistic foliar application of calcium, magnesium, and boron may represent an effective strategy for regulating fruit tree productivity by simultaneously improving mineral nutrition, photosynthetic performance, and assimilate allocation. Therefore, the combined foliar application of calcium (Ca), magnesium (Mg), and boron (B) holds considerable significance for yield formation in fruit trees.

Korla fragrant pear (*Pyrus sinkiangensis* Yü) is a distinctive and high-value pear cultivar originating from the Bayingol Mongolian Autonomous Prefecture of Xinjiang, China. This cultivar is highly appreciated for its unique flavor, thin peel, fine texture, crispness, juiciness, and rich nutritional composition, particularly its high vitamin C and mineral contents [14,15]. However, long-term orchard production of Korla fragrant pear has been associated with excessive and imbalanced fertilizer inputs, while insufficient attention to the balanced supply of secondary and micronutrients may increase the risk of nutrient imbalance and deficiency, thereby constraining further improvements in fruit quality and yield [16–18]. Currently, research on foliar fertilization in Korla fragrant pear has mainly focused on calcium nutrition, whereas systematic investigations into magnesium and boron nutrition, particularly their combined application with calcium, remain limited [19]. Consequently, the potential physiological mechanisms underlying Ca-Mg-B synergistic regulation of leaf growth and yield formation remain largely unexplored. Therefore, drawing on concentration ranges documented in previous studies, this study established a gradient of combined Ca-Mg-B foliar spray treatments to systematically evaluate the dose effects of this formulation on the leaf nutritional and physiological traits and yield of Korla fragrant pear, with the aim of identifying an optimal co-application concentration and providing a theoretical framework for precision fertilization and balanced nutrient management in Korla fragrant pear production.

## 2. Materials and Methods

### *2.1. Experimental Site Description*

The experiment was conducted in Awati Township, Korla City, Xinjiang Uygur Autonomous Region, China (86°4′ E, 41°41′ N). The experimental site is located at the southern foot of the Tianshan Mountains and the northeastern margin of the Tarim Basin, adjacent to the northern edge of the Taklimakan Desert. The region has a warm temperate continental arid climate, with an annual sunshine duration of approximately 2800–3100 h, mean annual temperature of 11.0–12.0 °C, annual precipitation of about 58 mm, annual evaporation of 2700–3000 mm, total solar radiation of 5600–6400 $MJ \cdot m^{-2}$, accumulated effective temperature of 4200–4500 °C, and a frost-free period of 210–240 d. Before the experiment, the soil nutrient status of the pear orchard was as follows: organic matter, 18.46 g $kg^{-1}$; total nitrogen, 0.91 g $kg^{-1}$; alkali-hydrolyzable nitrogen, 36.09 mg $kg^{-1}$; available phosphorus, 59.67 mg $kg^{-1}$; available potassium, 186.67 mg $kg^{-1}$; total calcium, 98.27 mg $g^{-1}$; total magnesium, 19.63 mg $g^{-1}$; total boron, 27.45 μg $g^{-1}$; and soil pH, 7.75.

### *2.2. Experimental Design*

The experiment was conducted continuously from 2024 to 2025 in a moderately fertile Korla fragrant pear (*Pyrus sinkiangensis* Yü) orchard. The experiment was initiated in 2024, and fertilizer treatments and sample collection were continued in 2025. The tested pear trees were 8–9 years old and grafted onto *Pyrus betulifolia* rootstock. The trees were planted at a spacing of 4 m × 1.5 m, and the actual surveyed planting density was 1500 plants $ha^{-1}$. The experiment was conducted using a randomized complete block design (RCBD). To minimize systematic variation associated with soil heterogeneity, the experimental field was divided into three blocks oriented along the drip-irrigation laterals. Each block included all four foliar-spray treatments, which were independently and completely randomized within the block. Each treatment within a block constituted a single experimental plot, yielding a total of 12 plots (4 treatments × 3 blocks). Each plot comprised five Korla fragrant pear trees with relatively uniform growth and no visible symptoms of disease or insect damage, all located within the same row. Based on the planting arrangement, the net plot area was approximately 30 $m^2$, with a within-row spacing of 1.5 m, a row length of 7.5 m for five consecutive trees, and a between-row spacing of 4.0 m. In total, 60 trees were included in the experiment. Within each plot, three trees were permanently tagged as fixed sampling trees. For each measured variable, equal quantities of material collected from the three tagged trees were pooled to form a single composite sample, and the corresponding measurement was treated as the observation for that plot. Thus, the experimental plot served as the statistical unit for all analyses, with three independent replicates per treatment ($n = 3$). Calcium, magnesium, and boron (Ca-Mg-B) fertilizers were applied as foliar sprays using an electric sprayer. Distilled water spraying was used as the control (CK), and three Ca-Mg-B foliar application concentrations were established: low concentration treatment (L-CaMgB), medium concentration treatment (M-CaMgB), and high concentration treatment (H-CaMgB). Calcium chloride ($CaCl_2$, Ca 36.11%), magnesium sulfate heptahydrate ($MgSO_4 \cdot 7H_2O$, Mg 9.86%), and boric acid ($H_3BO_3$, B 17.48%) were used as the sources of Ca, Mg, and B, respectively. Stock solutions were prepared separately with distilled water before application, mixed thoroughly immediately prior to spraying, and then applied as foliar spray without delay. The CK treatment received the same volume of distilled water. The elemental concentrations of the foliar solutions were as follows: L-CaMgB,0.1% Ca + 0.3% Mg + 0.15% B; M-CaMgB,0.2% Ca + 0.4% Mg + 0.25% B; and H-CaMgB,0.3% Ca + 0.5% Mg + 0.35% B. The applied concentrations represent the mass-to-volume concentrations of elemental Ca, Mg, and B, and the detailed application concentrations are presented in Table 1. The first foliar application was conducted on 30

June, followed by three additional applications at approximately 10-day intervals (10 July, 20 July, and 30 July). Foliar spraying was performed evenly on leaves and fruits under windless and sunny conditions until droplets appeared on the surface. The spray volume was maintained at 1500 mL per tree for each application to ensure complete wetting of both the adaxial and abaxial leaf surfaces. The basic fertilization regime in the experimental orchard included sheep manure (semi-decomposed farmyard manure), with total carbon, nitrogen, phosphorus, and potassium contents of 18.52%, 0.76%, 0.52%, and 0.45%, respectively. Sheep manure was applied once after fruit harvest in the previous autumn at a rate of 27,000 kg $ha^{-1}$ by broadcasting followed by soil incorporation. Nitrogen, phosphorus, and potassium fertilizers were applied during the annual growth period. Urea (N 46%) was applied at 40% as basal fertilizer before bud break and 60% as topdressing at different growth stages, including 20% during fruit set, 30% during the early fruit enlargement stage, and 10% during the late fruit enlargement stage. Calcium superphosphate ($P_2O_5$ 46%) was applied once as basal fertilizer before bud break. Potassium sulfate ($K_2O$ 51%) was applied with 40% as basal fertilizer before bud break and 60% as topdressing, including 10% during fruit set, 20% during the early fruit enlargement stage, and 30% during the late fruit enlargement stage. Basal fertilizers were applied using circular trench fertilization. Fertilizer trenches were established 50–80 cm from the trunk beneath the canopy, with a width of 30 cm and a depth of 30–60 cm. Nitrogen fertilizer topdressing was applied through drip fertigation using pressure-differential fertilizer tanks with a capacity of 15 L. Fertilizers were dissolved in water one day before each application. Other orchard management practices were consistent with local conventional practices.

**Table 1.** Concentration gradients of the combined Ca-Mg-B formulation for foliar application.

| Treatment | Ca-Mg-B |
|---|---|
| Control (CK) | 0-0-0 |
| Low concentration (L) | 0.1-0.3-0.15% |
| Medium concentration (M) | 0.2-0.4-0.25% |
| High concentration (H) | 0.3-0.5-0.35% |

### *2.3. Soil Sampling and Analysis*

Before the initiation of the experimental treatments in 2024, baseline soil samples were collected from the Korla fragrant pear orchard. After removing surface litter from both sides of the fertilization furrow in each treatment plot, soil samples were collected from the 0–20 cm layer using a soil auger. The three replicate plots of each treatment were sampled separately, and soil collected from both sides of the fertilization furrow within the same plot and soil layer was thoroughly homogenized to form one composite sample. In total, 12 soil samples were obtained (4 treatments × 3 replicates). The samples were air-dried at room temperature, cleared of stones, roots, and other debris, ground, passed through a 1 mm sieve, thoroughly mixed, and transferred into sample bottles before being sent to Nanjing Aoqing Biotechnology Co., Ltd. for analysis. After soil extraction, the concentrations of Ca and Mg ions in the extracts were determined using inductively coupled plasma mass spectrometry (ICP-MS).

### *2.4. Sample Collection and Processing*

Leaf samples were collected during the fruit enlargement stage (3 August). Three pear trees were randomly selected from each treatment. From each tree, fully expanded and healthy leaves with petioles were collected from the middle sections of current-year shoots at approximately 1.5–2.0 m above the ground in four directions (east, south, west, and north). In each direction, 2–5 leaves were collected, resulting in a total of 8–20 leaves

per tree. The collected leaves from each tree were pooled as one composite sample for subsequent analysis. During sampling, the collected leaves were consistent with those used for chlorophyll content determination. After collection, the leaves were gently rinsed with running tap water to remove surface dust and visible contaminants, followed by thorough washing with distilled water and sterile deionized water to minimize the influence of soluble mineral residues on the leaf surface. The petioles were sealed with wax, and the leaves were wrapped with plastic film, immediately placed into sealed bags, and transported on dry ice to Nanjing Aoqing Biotechnology Co., Ltd. for analysis. The concentrations of mineral elements, including nitrogen (N), phosphorus (P), potassium (K), calcium (Ca), magnesium (Mg), iron (Fe), manganese (Mn), copper (Cu), zinc (Zn), and boron (B), were determined. In addition, physiological and biochemical parameters were measured, including the activities of ribulose-1,5-bisphosphate carboxylase/oxygenase (Rubisco), peroxidase (POD), superoxide dismutase (SOD), catalase (CAT), phenylalanine ammonia-lyase (PAL), and polyphenol oxidase (PPO), as well as malondialdehyde (MDA) content and free proline (PRO) content.

Fruit samples were collected at the maturity stage (15 September). Before fruit sampling, yield measurements were conducted. For each fertilizer treatment, three tagged pear trees were selected for yield determination, and these trees were the same plants used for chlorophyll content and leaf area index measurements. Fruits were randomly collected from the east, south, west, and north directions of each tree across three canopy positions (upper, middle, and lower canopy layers). Four to seven fruits were collected from each canopy layer, resulting in a total of 20 fruits per tree. The harvested fruits were transported to the laboratory, where individual fruit weight was measured and yield-related parameters were calculated.

### *2.5. Determination of Physiological and Biochemical Parameters*

Leaf samples were first subjected to heat treatment at 105 °C for 30 min, followed by oven-drying at 80 °C to constant weight. The dried samples were ground using a stainless-steel grinder, passed through a 0.5 mm sieve, and stored in a cool, dry place until analysis. Total nitrogen (N) was determined using the Kjeldahl method [20]. Phosphorus (P), potassium (K), calcium (Ca), magnesium (Mg), iron (Fe), manganese (Mn), copper (Cu), zinc (Zn), and boron (B) were quantified following $HNO_3$–$H_2O_2$ digestion, adapted from Hansen (2009) [21]. Briefly, 0.2000 g of each sample was weighed into a digestion vessel, and 5 mL of high-purity $HNO_3$ was added for pre-digestion at 120 °C for 30 min. After cooling, 2 mL of $H_2O_2$ was added incrementally, and digestion was continued with gradual heating until a clear solution was obtained. The residual acid was removed by evaporation, and the digest was diluted to 50 mL with ultrapure water and filtered through a 0.45-μm membrane. Elemental concentrations were then determined using inductively coupled plasma mass spectrometry (ICP-MS). Germanium-72 ($^{72}$Ge), rhodium-103 ($^{103}$Rh), and rhenium-185 ($^{185}$Re) were used as internal standards to correct for matrix effects and signal drift. Potassium, calcium, and iron were measured using the collision/reaction cell in kinetic energy discrimination mode with helium (KED/He mode) to minimize polyatomic ion interferences, including $^{38}ArH^+$, $^{40}Ar^+$, and $^{40}Ar^{16}O^+$. Reagent blanks and replicate samples were included in each analytical batch. Quality control throughout the analytical procedure was performed using the certified reference material GBW10015 (GSB-6, spinach), with recovery rates for all elements maintained between 90% and 110%. For boron determination, a low-temperature digestion protocol not exceeding 120 °C was employed, and quartz or plastic vessels were used instead of borosilicate glassware to prevent boron loss and contamination.

Fresh leaf samples were weighed, thoroughly homogenized in the ice-cold extraction buffer supplied with the corresponding assay kit, and centrifuged at 4 °C under the conditions specified by the manufacturer. The resulting supernatants were collected for subsequent determination of enzyme activities and metabolite contents. All assays were performed in strict accordance with the manufacturers' instructions. All commercial assay kits were purchased from Nanjing Aoqing Biotechnology Co., Ltd. (Nanjing, Jiangsu, China). Ribulose-1,5-bisphosphate carboxylase/oxygenase (Rubisco) activity was determined spectrophotometrically according to the method described by Lilley and Walker [22], based on the decrease in absorbance at 340 nm resulting from NADH oxidation. A commercial NADH oxidation rate-based colorimetric assay kit (cat. no. GH6172; detection limit, 0.1 nmol $min^{-1}$ $g^{-1}$ FW) was used, and Rubisco activity was expressed as nmol $min^{-1}$ $g^{-1}$ FW. Superoxide dismutase (SOD) activity was determined using the WST-8 method with a commercial assay kit (cat. no. YH1200; detection limit, 1 U $g^{-1}$ FW) and expressed as U $g^{-1}$ FW. Peroxidase (POD) activity was measured using the guaiacol oxidation method with a commercial assay kit (cat. no. YH1210; detection limit, 1 U $g^{-1}$ FW) and expressed as U $g^{-1}$ FW. Catalase (CAT) activity was determined using the ammonium molybdate colorimetric method with a commercial assay kit (cat. no. YH1206; detection limit, 1 μmol $min^{-1}$ $g^{-1}$ FW) and expressed as μmol $min^{-1}$ $g^{-1}$ FW.

Malondialdehyde (MDA) content was quantified using the thiobarbituric acid (TBA) colorimetric method with a commercial assay kit (cat. no. YH1217; detection limit, 1 nmol $g^{-1}$ FW) and expressed as nmol $g^{-1}$ FW. Free proline (PRO) content was determined using the sulfosalicylic acid–acidic ninhydrin colorimetric method with a commercial assay kit (cat. no. YH1231; detection limit, 1 μg $g^{-1}$ FW) and expressed as μg $g^{-1}$ FW. Phenylalanine ammonia-lyase (PAL) activity was assayed by ultraviolet spectrophotometry using L-phenylalanine as the substrate, with absorbance monitored at 290 nm. A commercial PAL assay kit (cat. no. YH1227; detection limit, 0.78 U $g^{-1}$ FW) was used, and PAL activity was expressed as U $g^{-1}$ FW. Polyphenol oxidase (PPO) activity was determined using the catechol oxidation method, with absorbance monitored at 398 nm. A commercial PPO assay kit (cat. no. YH1223; detection limit, 1 U $g^{-1}$ FW) was used, and PPO activity was expressed as U $g^{-1}$ FW. FW denotes fresh weight.

Chlorophyll content: The relative chlorophyll content of pear leaves was measured using a SPAD-502 chlorophyll meter (Konica Minolta, Tokyo, Japan). Five fully expanded and healthy leaves were randomly selected from each tree, and the mean value was calculated as the chlorophyll content of each plant.

Leaf area index (LAI): Leaf area index was measured directly in the field using an AccuPARLP-80 PAR/LAI Ceptometer (METER Group, Pullman, WA, USA). Measurements were conducted on 3 August under clear, windless conditions during the period of high solar elevation (12:00–16:00, Beijing Time). For each tree, measurements were performed at four fixed positions corresponding to the east, south, west, and north directions. The mean value of the four measurements was calculated and used as the LAI value for each tree.

Yield determination: The yield per tree was calculated by multiplying the total number of fruits per tree by the average fruit weight. The yield per hectare was subsequently calculated by multiplying the yield per tree by the number of trees per hectare.

### *2.6. Data Analysis*

Experimental data were organized and preliminarily processed using Microsoft Excel 2020, and statistical analyses were performed with SPSS 26.0. For data satisfying the assumptions of normality and homogeneity of variance, differences among treatments were evaluated by one-way analysis of variance (ANOVA), followed by Tukey's honestly significant difference (HSD) test for post hoc pairwise comparisons; different lowercase letters in the figures denote significant differences among treatments ($p < 0.05$). For data violating these assumptions, the Kruskal–Wallis test was employed, followed by Dunn's test for post hoc multiple comparisons. All results are expressed as means ± standard error (SE). Bar charts were generated with Origin 2021; Mantel test and correlation analysis results were visualized using the Genescloud platform; the Pearson correlation heatmap was constructed with R software (version 4.4.3); and structural equation modeling (SEM) was conducted using SmartPLS 4.1.1.8, with final graphical refinement and layout performed in WPS Office PowerPoint.

## 3. Results

### *3.1. Effects of Ca-Mg-B Foliar Application on Macronutrient Contents in Korla Fragrant Pear Leaves*

As shown in Figure 1, compared with CK, leaf N, P, and K contents generally followed a "rise-then-decline" trend with increasing Ca-Mg-B spray concentration, indicating that an appropriate Ca-Mg-B concentration enhances the uptake efficiency of these macronutrients. Leaf N content differed significantly from CK under all Ca-Mg-B treatments; P content differed significantly under the L and M treatments but not under the H treatment; and K content differed significantly only under the M treatment. Relative to CK, foliar application of L, M, and H Ca-Mg-B significantly increased leaf N content by 19.15%, 59.09%, and 38.52%, respectively, and P content by 14.96%, 21.04%, and 8.80%, respectively, whereas K content increased by 16.56% and 49.38% under the L and M treatments but decreased by 9.19% under the H treatment. The promotion of leaf N, P, and K accumulation peaked under the medium-concentration Ca-Mg-B treatment, demonstrating the existence of a concentration threshold for Ca-Mg-B application, beyond which nutrient uptake declines.

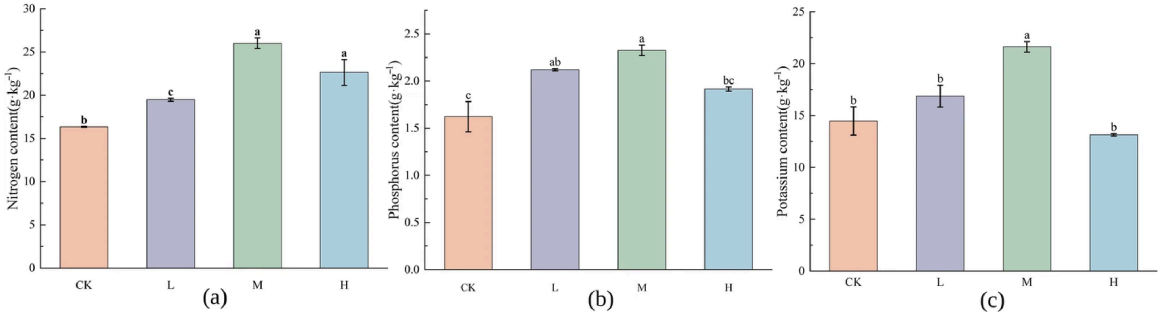



**Figure 1.** Effects of Ca-Mg-B application on macronutrient contents in leaves of Korla fragrant pear. (**a**–**c**) represent nitrogen (N), phosphorus (P), and potassium (K) contents, respectively. Data are presented as means ± SE of three replicate plots ($n = 3$), with each plot comprising five trees; the plot was treated as the experimental unit. Different lowercase letters indicate significant differences among treatments ($p < 0.05$).

### *3.2. Effects of Ca-Mg-B Foliar Application on Secondary Macronutrient Contents in Korla Fragrant Pear Leaves*

As shown in Figure 2, compared with CK, foliar application of Ca-Mg-B at all concentrations promoted Ca and Mg uptake in Korla fragrant pear leaves, with the greatest

promotion observed under the M treatment. Leaf Ca content differed significantly from CK under the L and M treatments, whereas Mg content differed significantly under all treatments. Relative to CK, leaf Ca content increased by 45.89%, 51.41%, and 27.43% under the L, M, and H treatments, respectively, while Mg content increased significantly by 16.65%, 40.27%, and 26.22%, respectively. Overall, leaf Ca and Mg contents exhibited a "rise-then-decline" pattern with increasing Ca-Mg-B spray concentration, indicating that an appropriate Ca-Mg-B concentration facilitates Ca and Mg uptake, whereas excessive concentrations reduce their absorption in leaves.

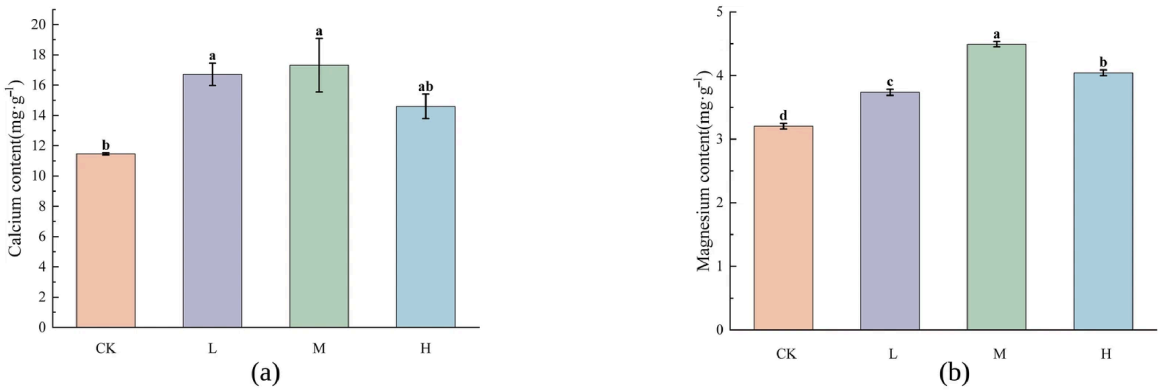



**Figure 2.** Effects of Ca-Mg-B application on secondary macronutrient contents in leaves of Korla fragrant pear. (**a**) and (**b**) represent calcium (Ca) and magnesium (Mg) contents, respectively. Data are presented as means ± SE of three replicate plots ($n = 3$), with each plot comprising five trees; the plot was treated as the experimental unit. Different lowercase letters indicate significant differences among treatments ($p < 0.05$).

### *3.3. Effects of Ca-Mg-B Foliar Application on Micronutrient Contents in Korla Fragrant Pear Leaves*

As shown in Figure 3, relative to the CK treatment, foliar application of Ca–Mg–B across all concentration gradients elevated the contents of Mn, Cu, Zn, and B, with the M treatment consistently yielding the most pronounced effect. Leaf Mn content was significantly higher under the M and H treatments than under CK, whereas a significant increase in Cu content was observed only under the M treatment. Leaf Zn content was significantly higher under all Ca-Mg-B treatments than under CK, while a significant increase in B content was observed under the M treatment. Compared with CK, foliar application of Ca-Mg-B at L, M, and H concentrations increased leaf Mn content by 30.05%, 73.53%, and 42.59%, respectively. Similarly, leaf Cu content increased by 21.45%, 53.29%, and 24.81%, respectively, while Zn content increased by 11.77%, 26.35%, and 11.40%, respectively. The corresponding increases in leaf B content were 39.27%, 160.73%, and 40.55%, respectively. In contrast, leaf Fe content decreased progressively with increasing Ca-Mg-B concentration, declining by 6.24%, 14.83%, and 29.52% under the L, M, and H treatments, respectively, relative to CK. Overall, these results indicate that Ca-Mg-B foliar application at an appropriate concentration promoted the accumulation of Mn, Cu, Zn, and B in Korla fragrant pear leaves, whereas increasing Ca-Mg-B concentration exerted an inhibitory effect on Fe accumulation. The M treatment consistently produced the strongest positive response for Mn, Cu, Zn, and B, suggesting that the medium Ca-Mg-B concentration was most effective in improving the micronutrient status of Korla fragrant pear leaves.

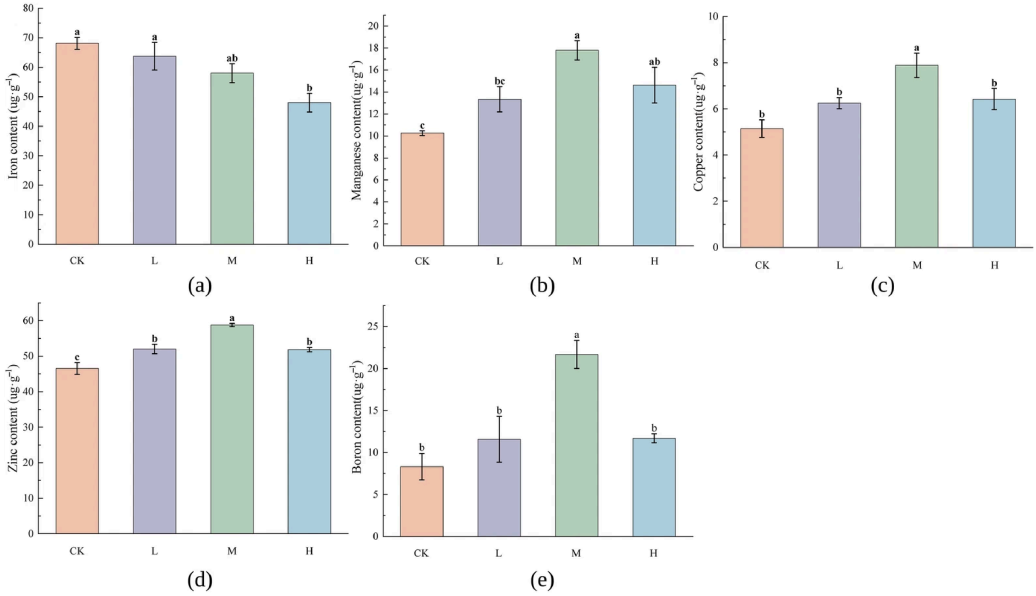



**Figure 3.** Effects of Ca-Mg-B application on micronutrient contents in leaves of Korla fragrant pear. (**a**), (**b**), (**b**), (**d**) and (**e**) represent iron (Fe), manganese (Mn), copper (Cu), zinc (Zn), and boron (B) contents, respectively. Data are presented as means ± SE of three replicate plots ($n = 3$), with each plot comprising five trees; the plot was treated as the experimental unit. Different lowercase letters indicate significant differences among treatments ($p < 0.05$).

### *3.4. Effects of Ca-Mg-B Foliar Application on Chlorophyll Content and Leaf Area Index in Korla Fragrant Pear Leaves*

As shown in Figure 4, foliar application of Ca-Mg-B at different concentrations increased SPAD values and leaf area index (LAI) compared with the CK treatment, with both parameters showing an overall pattern of an initial increase followed by a decrease as the application concentration increased. Compared with CK, Ca-Mg-B application at L, M, and H concentrations significantly increased SPAD values by 18.59%, 20.01%, and 17.09%, respectively. SPAD values were significantly higher under all Ca-Mg-B treatments than under CK, whereas no significant differences were observed among the three Ca-Mg-B concentrations. Leaf area index increased by 5.75%, 47.88%, and 8.75% under the L, M, and H treatments, respectively, relative to CK, with a significant difference observed only between the M and CK treatments. Both SPAD and LAI showed the strongest responses under the M treatment, whereas their values tended to decrease under the H treatment. These results indicate that the effects of Ca-Mg-B foliar application on chlorophyll status and canopy development were concentration-dependent, with the medium concentration providing the greatest improvement, while excessive Ca-Mg-B application weakened these beneficial effects.

Mantel tests were employed to assess the associations of SPAD and LAI with leaf mineral element concentrations, whereas Pearson correlation analysis was used to examine pairwise relationships among individual mineral elements (Figure 5). LAI exhibited the strongest association with B ($r = 0.893$, $p < 0.001$) and was also significantly correlated with N ($r = 0.780$), K ($r = 0.779$), P ($r = 0.729$), Mn ($r = 0.724$), Cu ($r = 0.684$), Ca ($r = 0.638$), and Zn ($r = 0.590$). By contrast, its associations with Mg and Fe were not statistically significant. SPAD was significantly correlated with N ($r = 0.695$), Ca ($r = 0.726$), Cu ($r = 0.721$), Mn ($r = 0.687$), and P ($r = 0.649$), whereas no significant associations were detected with K, Zn, B, Mg, or Fe. Overall, LAI was significantly associated with a broader range of mineral elements than SPAD. Pearson correlation analysis revealed numerous significant positive relationships among N, P, K, Ca, Mn, Cu, Zn, and B (Figure 5). The strongest correlation

was observed between N and Mn (r = 0.888), followed by Mn–B (r = 0.794), K–B (r = 0.788), P–B (r = 0.785), and N–B (r = 0.770). In contrast, neither Mg nor Fe exhibited significant correlations with the other mineral elements. Collectively, these findings demonstrate significant statistical associations between LAI and SPAD and selected mineral elements, as well as among several mineral nutrients. These correlation analyses are presented as exploratory assessments of association patterns among the measured variables.

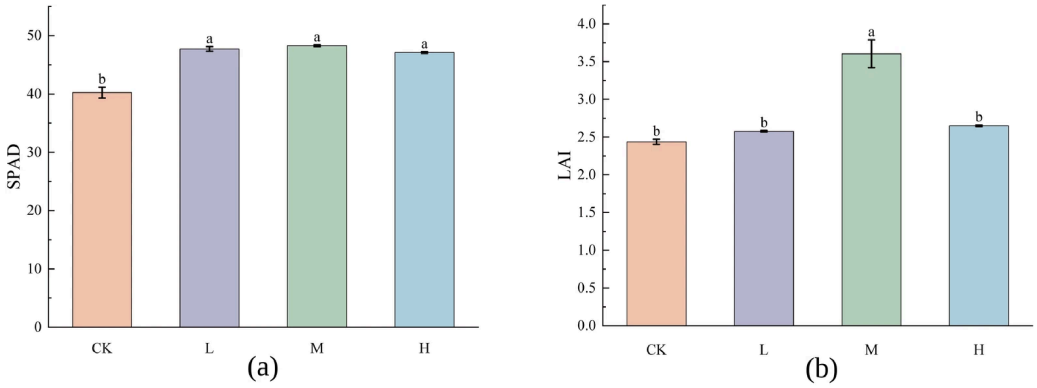



**Figure 4.** Effects of Ca-Mg-B application on photosynthesis-related traits in leaves of Korla fragrant pear. (**a**) and (**b**) represent chlorophyll content (SPAD value) and leaf area index (LAI), respectively. Data are presented as means ± SE of three replicate plots ($n = 3$), with each plot comprising five trees; the plot was treated as the experimental unit. Different lowercase letters indicate significant differences among treatments ($p < 0.05$).

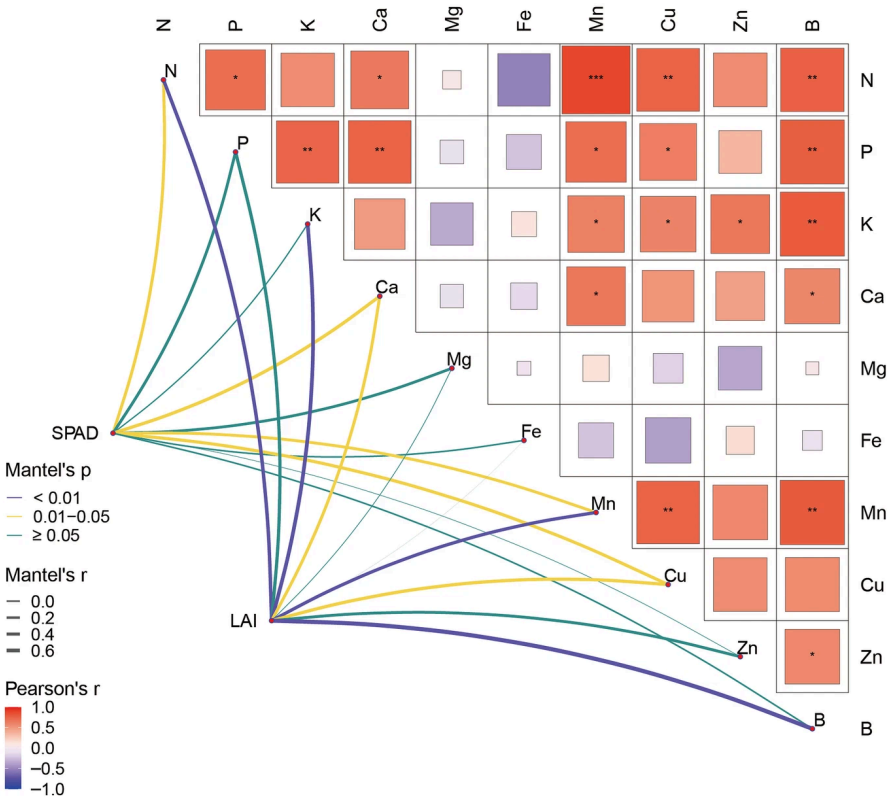



**Figure 5.** Correlations between leaf mineral nutrient contents and photosynthesis-related traits (SPAD value and leaf area index, LAI) in Korla fragrant pear following Ca-Mg-B application. SPAD represents the relative chlorophyll content expressed as SPAD value, and LAI represents leaf area index. * indicates a significant correlation ($p < 0.05$), whereas ** and *** indicate highly significant correlations ($p < 0.01$ and $p < 0.001$, respectively). $n = 12$.

### *3.5. Effects of Ca-Mg-B Foliar Application on Physiological and Biochemical Parameters in Korla Fragrant Pear Leaves*

As shown in Figure 6, Rubisco activity in Korla fragrant pear leaves differed significantly among Ca-Mg-B treatments and CK and exhibited an overall pattern of an initial increase followed by a decrease with increasing Ca-Mg-B application concentration. Compared with CK, Ca-Mg-B application at L, M, and H concentrations significantly increased Rubisco activity by 104.55%, 171.41%, and 95.90%, respectively, with the greatest increase observed under the M treatment. These results indicate that an appropriate Ca-Mg-B concentration enhanced Rubisco activity, whereas the promoting effect was weakened at the H concentration. Compared with CK, the activities of superoxide dismutase (SOD), peroxidase (POD), and catalase (CAT) in Korla fragrant pear leaves increased to varying degrees following Ca-Mg-B application. POD activity initially increased and subsequently declined with increasing Ca-Mg-B concentration, with the strongest response observed under the L treatment. In contrast, SOD and CAT activities exhibited an initial increase followed by a decrease. Compared with CK, Ca-Mg-B application at L, M, and H concentrations increased SOD activity by 48.40%, 127.26%, and 47.79%, respectively, although a significant difference was observed only between the M and CK treatments. POD activity increased by 67.57%, 37.75%, and 14.42%, respectively, with a significant difference observed only between the L and CK treatments. CAT activity increased by 42.59%, 128.90%, and 61.84%, respectively, and the M and H treatments differed significantly from CK. Notably, SOD, POD, and CAT activities all declined under the H treatment relative to their respective lower-concentration treatments, indicating that the beneficial effects of Ca-Mg-B on antioxidant enzyme activities were attenuated at excessive concentrations. The increase in SOD activity under H was slightly lower than that under L, whereas the increase in CAT activity remained higher than that under L, suggesting differential responses of the three antioxidant enzymes to the Ca-Mg-B concentration gradient.

Ca-Mg-B application also significantly affected the activities of phenylalanine ammonia-lyase (PAL) and polyphenol oxidase (PPO), with the most pronounced regulatory effects observed under the M treatment. PAL activity exhibited an initial increase followed by a decrease with increasing Ca-Mg-B concentration, whereas PPO activity showed a fluctuating response. Compared with CK, Ca-Mg-B application at L, M, and H concentrations increased PAL activity by 19.07%, 79.31%, and 1.39%, respectively. PPO activity increased by 18.13% and 3.31% under the L and H treatments, respectively, but decreased significantly by 30.67% under the M treatment. PAL activity showed the greatest increase under the M treatment, whereas PPO activity showed the strongest decrease under the same treatment. The regulatory effects on both enzymes were attenuated under the H treatment. These results indicate that an appropriate Ca-Mg-B concentration enhanced PAL activity while suppressing PPO activity, whereas excessive application weakened these responses. Compared with CK, Ca-Mg-B application at different concentrations significantly affected the contents of malondialdehyde (MDA) and proline (PRO) in Korla fragrant pear leaves. MDA content decreased continuously with increasing Ca-Mg-B concentration, whereas PRO content showed a continuous increasing trend. Relative to CK, Ca-Mg-B application at L, M, and H concentrations decreased MDA content by 5.52%, 21.33%, and 26.47%, respectively, while increasing PRO content by 2.93%, 17.61%, and 68.91%, respectively. The concurrent decrease in MDA and increase in PRO suggest coordinated changes in membrane lipid peroxidation and osmotic adjustment following Ca-Mg-B application. The pronounced accumulation of PRO under the H treatment may indicate an altered osmotic status under excessive Ca-Mg-B application.

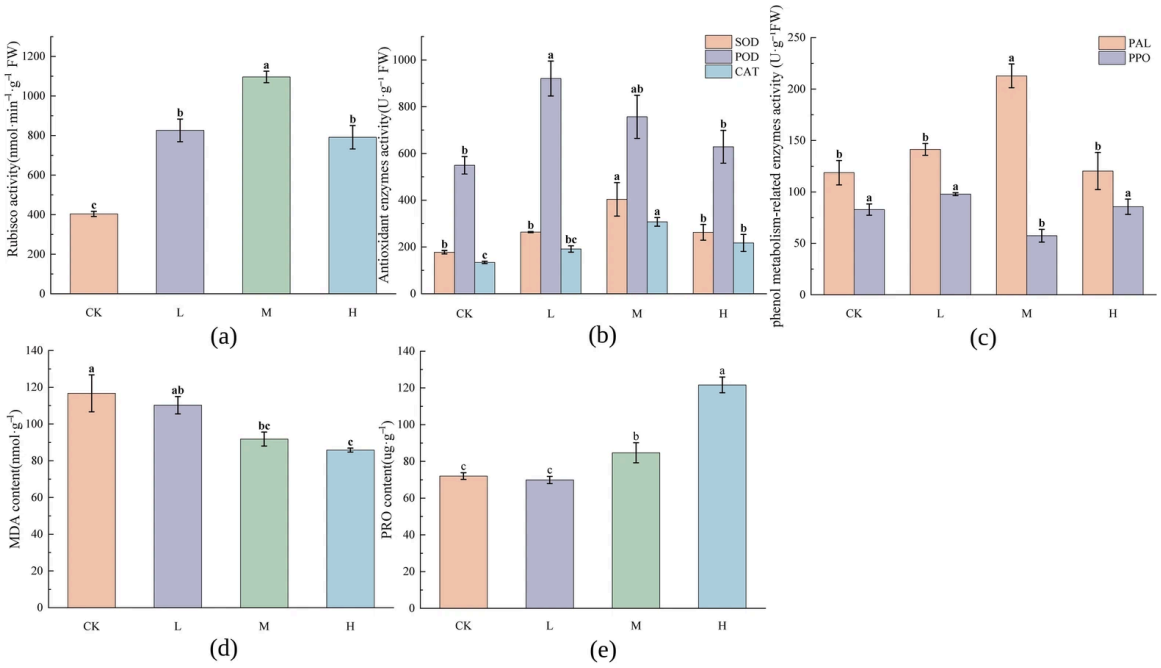



**Figure 6.** Effects of Ca-Mg-B application on physiological and biochemical traits in leaves of Korla fragrant pear. (**a**) represents ribulose-1,5-bisphosphate carboxylase/oxygenase (Rubisco) activity; (**b**) represents antioxidant enzyme activities, including peroxidase (POD), superoxide dismutase (SOD), and catalase (CAT); (**c**) represents secondary metabolism-related enzyme activities, including phenylalanine ammonia-lyase (PAL) and polyphenol oxidase (PPO); (**d**) represents malondialdehyde (MDA) content; and (**e**) represents free proline (PRO) content. Data are presented as means ± SE of three replicate plots ($n = 3$), with each plot comprising five trees; the plot was treated as the experimental unit. Different lowercase letters indicate significant differences among treatments ($p < 0.05$).

Pearson correlation analysis was conducted to examine the relationships between leaf mineral element concentrations and physiological and biochemical traits, including POD, CAT, SOD, PAL, and PPO activities, Rubisco activity, and MDA and PRO contents (Figure 7). The analysis was based on 12 plot-level observations across four treatment levels ($n = 12$). Because some of the observed correlations may partly reflect the shared treatment gradient, these results are presented as an exploratory assessment of association patterns among the measured variables. CAT, SOD, PAL, and Rubisco activities were significantly and positively associated with multiple mineral elements ($p < 0.05$). CAT activity was positively correlated with N (r = 0.91), Mn (r = 0.91), Cu (r = 0.79), Ca (r = 0.77), B (r = 0.75), P (r = 0.73), Zn (r = 0.62), and K (r = 0.61). SOD activity was positively correlated with Mn (r = 0.88), N (r = 0.82), Cu (r = 0.80), Zn (r = 0.80), B (r = 0.70), K (r = 0.68), P (r = 0.61), and Ca (r = 0.59). PAL activity was positively associated with K (r = 0.85), N (r = 0.74), Cu (r = 0.71), Zn (r = 0.69), B (r = 0.69), P (r = 0.68), and Mn (r = 0.64). Rubisco activity was positively correlated with N (r = 0.88), P (r = 0.86), Ca (r = 0.80), B (r = 0.77), Mn (r = 0.74), Cu (r = 0.74), and K (r = 0.64). By contrast, PPO activity was significantly and negatively correlated only with B (r = −0.74). MDA content was negatively associated with N (r = −0.70) and Mn (r = −0.69), whereas PRO content showed a significant negative correlation only with Fe (r = −0.74). POD activity was not significantly correlated with any mineral element ($p > 0.05$). Similarly, Mg showed no significant association with any of the physiological or biochemical traits examined ($p > 0.05$). Except for its negative correlation with PRO, Fe was not significantly associated with any of the remaining physiological or biochemical variables ($p > 0.05$).

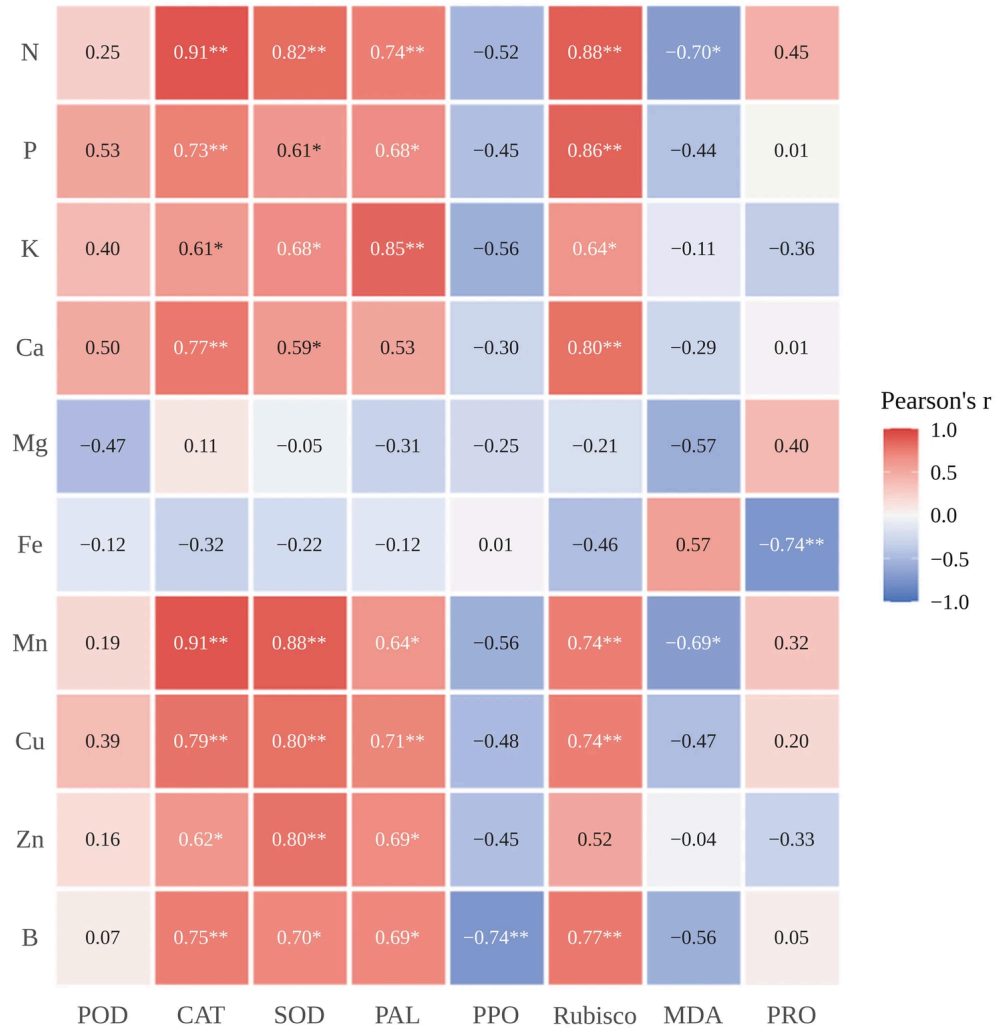



**Figure 7.** Pearson correlation heatmap between leaf mineral nutrient contents and physiological and biochemical traits in Korla fragrant pear following Ca-Mg-B application. The color scale represents the Pearson correlation coefficient (r), with red and blue indicating positive and negative correlations, respectively. The numbers in the heatmap indicate Pearson correlation coefficients (r). Asterisks indicate the significance levels of correlations: * indicates significant correlation ($p < 0.05$), and ** indicates extremely significant correlation ($p < 0.01$). Correlation analysis was performed based on 12 independent observations ($n = 12$). POD, peroxidase; CAT, catalase; SOD, superoxide dismutase; PAL, phenylalanine ammonia-lyase; PPO, polyphenol oxidase; Rubisco, ribulose-1,5-bisphosphate carboxylase/oxygenase; MDA, malondialdehyde; PRO, free proline.

### *3.6. Effects of Ca-Mg-B Foliar Application on Fruit Yield of Korla Fragrant Pear*

As shown in Table 2, compared with the CK treatment, foliar application of Ca-Mg-B at all concentrations significantly increased fruit weight, with the L, M, and H treatments increasing fruit weight by 20.58%, 36.78%, and 15.10%, respectively, the M treatment being the most effective. As the Ca-Mg-B application concentration increased, the fruit weight of fragrant pear exhibited an initial increase followed by a decrease, indicating that an appropriate Ca-Mg-B concentration promoted fruit enlargement and the formation of fruit weight. No significant differences were detected among individual trees. Regarding yield per tree, the M treatment differed significantly from the CK treatment and achieved the highest yield per tree, although it did not differ significantly from the L and H treatments. With increasing Ca-Mg-B application concentration, the yield per tree of fragrant pear showed a trend of initial increase followed by decrease, suggesting that appropriate Ca-Mg-B application benefits the mineral nutrient balance of pear trees, thereby increasing

yield per tree. Compared with the CK treatment, the L, M, and H treatments increased yield per tree by 10.75%, 33.65%, and 5.87%, respectively; the relatively small increment under the H treatment indicates that the yield-promoting effect was constrained at higher application concentrations. In terms of yield, the M treatments differed significantly from the CK treatment, and fruit yield likewise exhibited a trend of initial increase followed by decrease with increasing Ca-Mg-B concentration, indicating that an appropriate Ca-Mg-B concentration promoted yield formation. Compared with the CK treatment, the L, M, and H treatments increased fruit yield by 10.77%, 33.78%, and 5.03%, respectively; given that the H treatment was less effective than the L treatment, these results suggest that a concentration threshold exists for Ca-Mg-B foliar application, beyond which the yield increment declines.

**Table 2.** Effects of different concentrations of Ca-Mg-B foliar fertilizer on fruit weight, yield per tree, and yield of Korla fragrant pear.

| Treatment | Single Fruit Weight (g) | Fruit Number Per Tree | Yield Per Fruit Tree (kg Tree$^{-1}$) | Yield (kg ha$^{-1}$) |
|---|---|---|---|---|
| CK | 152.33 ± 4.67 c | 152.2 ± 2.7 a | 23.16 ± 0.45 b | 34,740.25 ± 678.70 b |
| L | 183.67 ± 3.71 b | 139.6 ± 3.4 a b | 25.65 ± 1.01 b | 38,480.2 ± 1509.60 b |
| M | 208.33 ± 6.06 a | 148.8 ± 1.6 a b | 30.98 ± 0.80 a | 46,476.8 ± 1204.60 a |
| H | 175.33 ± 3.48 b | 139.0 ± 6.0 b | 24.32 ± 0.60 b | 36,486.85 ± 898.12 b |

Data are presented as the mean ± standard error (SE) of three independent replicate plots ($n = 3$), with the plot treated as the experimental unit. Each replicate plot comprised five trees, all of which received the same treatment. Different lowercase letters indicate significant differences among treatments ($p < 0.05$).

To characterize the association patterns among leaf mineral nutrition, physiological traits, and yield components under Ca–Mg–B treatments, exploratory Pearson correlation analyses and Mantel tests were conducted across all measured variables (Figure 8). Mantel tests revealed significant associations among all three variable groups. The strongest relationship was observed between mineral nutrition and leaf physiological traits (r = 0.85, $p < 0.001$), followed by that between physiological traits and yield components (r = 0.75, $p < 0.001$) and between mineral nutrition and yield components (r = 0.68, $p < 0.001$). The Pearson correlation matrix further showed that CAT, SOD, PAL, and Rubisco activities were each significantly and positively associated with multiple mineral elements. Particularly strong correlations were observed for N–CAT (r = 0.91), Mn–CAT (r = 0.91), N–Rubisco (r = 0.88), P–Rubisco (r = 0.86), and K–PAL (r = 0.85). PPO activity was significantly and negatively correlated with B (r = −0.74), whereas MDA content was negatively correlated with N (r = −0.70) and Mn (r = −0.69). PRO content was significantly and negatively associated with Fe (r = −0.74), while no significant correlations were detected between POD activity and any mineral element. All three yield-related traits were significantly and positively correlated with one another ($p < 0.001$). Yield showed particularly strong positive correlations with LAI (r = 0.918), PAL activity (r = 0.884), CAT activity (r = 0.858), and Rubisco activity (r = 0.844), and was also significantly and positively associated with Cu, P, N, B, K, Ca, SOD activity, Mn, and Zn. In contrast, PPO activity was significantly and negatively correlated with yield (r = −0.653), whereas Mg, Fe, POD, MDA, and PRO showed no significant associations with yield. Overall, mineral nutrition, physiological traits, and yield components exhibited extensive statistical associations across the Ca–Mg–B treatments. Because these analyses were based on 12 plot-level observations across four treatment levels, some of the observed relationships may partly reflect the shared treatment gradient. Accordingly, the results are presented as an exploratory assessment of coordinated variation among the measured traits.

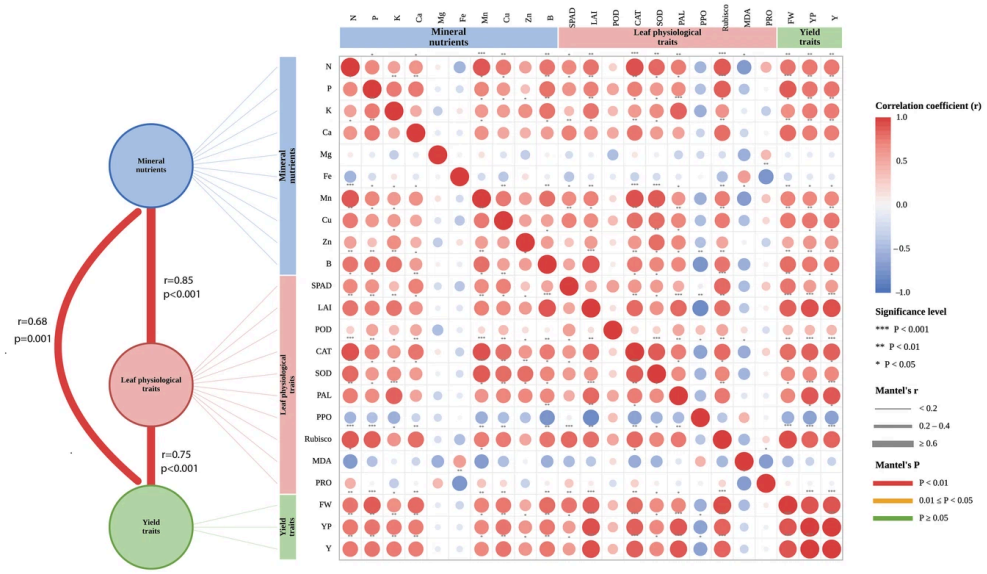



**Figure 8.** Integrated correlation analysis of leaf mineral nutrients, physiological traits, and yield characteristics of Korla fragrant pear under Ca-Mg-B foliar application. (Left) Mantel test results among different groups of indicators. The line width represents Mantel's r, and line color indicates the significance level (red, $p < 0.01$; orange, $0.01 \leq p < 0.05$; green, $p \geq 0.05$). The exact Mantel r and $p$ values are shown next to each connection. (Right) Pearson correlation coefficients among individual indicators. Circle size and color represent the correlation coefficient, with red indicating positive correlations and blue indicating negative correlations. Asterisks indicate significance levels (* $p < 0.05$, ** $p < 0.01$, *** $p < 0.001$). FW, fruit weight; YP, yield per tree; Y, yield. $n = 12$.

### *3.7. PLS-SEM Analysis of the Effects of Ca-Mg-B Foliar Application on Leaf Growth Traits and Fruit Yield of Korla Fragrant Pear*

To examine the relationships among leaf mineral nutrition, LAI, SPAD, antioxidant enzyme activity, non-enzymatic stress indicators, Rubisco activity, and Korla fragrant pear yield across different Ca–Mg–B concentration treatments, a PLS-SEM model was constructed with yield as the final response variable (Figure 9). The model revealed a significant positive path from Ca–Mg–B treatment to leaf mineral nutrient status ($\beta = 0.661$, $p < 0.01$). Leaf mineral nutrient status was strongly and positively associated with both LAI and SPAD, with path coefficients of 0.863 and 0.756, respectively (both $p < 0.001$). The model explained 74.5% and 57.2% of the variance in LAI and SPAD, respectively. In the measurement model, N, P, K, Ca, Mn, Cu, Zn, and B exhibited standardized loadings ranging from 0.640 to 0.925 on the latent variable representing leaf mineral nutrient status. The structural model further indicated a strong positive relationship between LAI and antioxidant enzyme activity ($\beta = 0.777$, $p < 0.001$), whereas the path from SPAD to antioxidant enzyme activity was weaker and not statistically significant ($\beta = 0.195$). SPAD was negatively associated with non-enzymatic stress indicators ($\beta = -0.490$), while the path coefficient between LAI and non-enzymatic stress indicators was −0.103. Antioxidant enzyme activity was strongly and positively associated with Rubisco activity ($\beta = 0.775$, $p < 0.001$), whereas non-enzymatic stress indicators were negatively associated with Rubisco activity ($\beta = -0.182$). Rubisco activity, in turn, showed a strong positive association with Korla fragrant pear yield ($\beta = 0.844$, $p < 0.001$). The model explained 72.5% of the variance in Rubisco activity and 71.2% of the variance in yield. Overall, the PLS-SEM results identified multiple direct and indirect statistical pathways linking Ca–Mg–B treatment, leaf mineral nutrient status, LAI, SPAD, antioxidant enzyme activity, non-enzymatic stress indicators, Rubisco activity, and yield. Significant or highly significant positive paths were observed from mineral nutrient status to LAI and SPAD, from LAI to antioxidant enzyme activity, from antioxidant enzyme

activity to Rubisco activity, and from Rubisco activity to yield. Given that the model was based on only 12 plot-level observations, these path coefficients should be interpreted as exploratory findings.

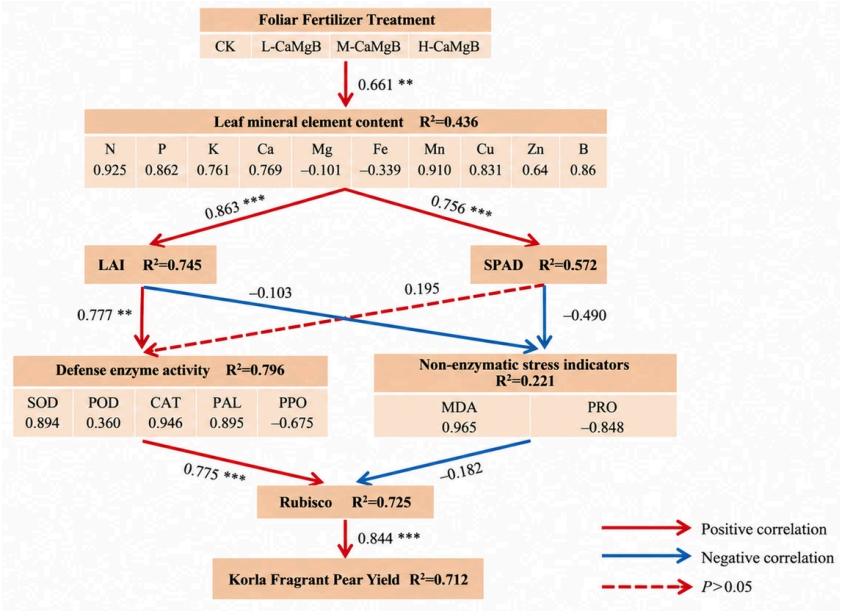



**Figure 9.** Partial least squares structural equation model (PLS-SEM) revealing the pathways by which Ca-Mg-B foliar application regulates leaf mineral nutrient status, enzyme activities, photosynthesis-related parameters, and yield formation in Korla fragrant pear. Arrows indicate the hypothesized causal paths among latent variables, and the values on the arrows are standardized path coefficients (β). $R^2$ values represent the proportion of variance explained in each endogenous latent variable. Solid and dashed arrows indicate significant and non-significant paths, respectively (** $p < 0.01$, *** $p < 0.001$). SPAD, soil and plant analyzer development chlorophyll index; LAI, leaf area index; SOD, superoxide dismutase; POD, peroxidase; CAT, catalase; PAL, phenylalanine ammonia-lyase; PPO, polyphenol oxidase; Rubisco, ribulose-1,5-bisphosphate carboxylase/oxygenase; MDA, malondialdehyde; PRO, proline.

## 4. Discussion

### *4.1. Effects of Ca-Mg-B Foliar Application on Mineral Element Concentrations in Korla Fragrant Pear*

Foliar application of appropriate secondary and micronutrients can significantly promote nutrient uptake and mineral element accumulation in fruit tree leaves, thereby improving photosynthetic efficiency and stress tolerance and ultimately enhancing fruit yield [23,24]. The fruit enlargement stage represents a critical period of fruit development characterized by particularly high mineral nutrient requirements. As essential nutrients for plant growth and development, calcium (Ca), magnesium (Mg), and boron (B) may exert synergistic effects that directly influence the uptake, translocation, and allocation of mineral nutrients in pear trees. In the present study, Ca-Mg-B foliar application significantly increased leaf B concentration, with the M treatment showing a 160.73% increase compared with CK, and simultaneously promoted the accumulation of multiple mineral elements, including N, P, K, Ca, Mg, Mn, and Zn. Vera-Maldonado et al. [25] pointed out that B can interact with multiple mineral nutrients and may indirectly influence their uptake and utilization through the regulation of related physiological and molecular networks. This is consistent with our findings, suggesting that an adequate B supply may facilitate coordinated mineral nutrient accumulation and contribute to improved overall nutritional status in pear leaves. In the present study, the concentrations of N, P, K, Ca, Mg,

Mn, Cu, Zn, and B in pear leaves exhibited an increase–decrease pattern with increasing Ca-Mg-B application concentration, indicating that foliar Ca-Mg-B application exerted a clear dose-dependent effect on leaf mineral nutrition and that an appropriate application level may be more conducive to maintaining mineral nutrient balance in leaves. Similarly, Abobatta et al. [23] reported that different foliar fertilizer application rates and combinations resulted in differential growth and productivity responses in Navel orange, allowing a more favorable application level to be identified. Moreover, an appropriate Ca-Mg-B concentration promoted the accumulation of multiple mineral elements, including N, P, K, Ca, Mg, Mn, Cu, Zn, and B. This result is consistent with the findings of Al-Dulaimi and Alrawi [26] in apple and Mutlag et al. [27] in 'Coscia' pear, both of which demonstrated that appropriate foliar nutrient concentrations could enhance the uptake and accumulation of multiple mineral elements. These findings collectively indicate that the effects of Ca-Mg-B foliar application extend beyond the accumulation of the applied nutrients themselves and may involve broader regulation of mineral nutrient homeostasis in leaves. In the present study, leaf K content declined by 9.97% under the H treatment; however, this reduction was not statistically significant, suggesting that the H-CaMgB treatment did not substantially impede K uptake. This modest decline is more plausibly attributable to the regulation of cation homeostasis within the plant. As essential inorganic cations, $Ca^{2+}$, $Mg^{2+}$ and $K^{+}$ engage in intricate interactions during root acquisition, long-distance translocation and foliar partitioning, and plants sustain intracellular ion homeostasis by fine-tuning ion transport and allocation [28]. Furthermore, although Mg and K frequently act synergistically, their relationship is also modulated by shifts in ionic ratios; an enhanced exogenous Mg supply may prompt plants to preserve mineral balance through adjustment of the K/Mg ratio, thereby inducing a degree of fluctuation in leaf K content [28]. In addition, Fe content exhibited a declining trend with increasing Ca–Mg–B concentration: the reductions under the L and M treatments were non-significant, whereas the H treatment elicited a significant decrease, a pattern likely arising from the combined constraints of limited soil Fe availability and a growth-mediated dilution effect. Under high-pH conditions, $Fe^{3+}$ readily precipitates as sparingly soluble oxides and hydroxides, thereby restricting both root Fe acquisition and its translocation to the shoots [29]. Concurrently, the H-CaMgB treatment stimulated leaf expansion and biomass accumulation, potentially giving rise to a dilution effect in which the rate of dry matter accumulation outpaced that of Fe uptake, ultimately lowering Fe concentration per unit leaf mass [30].

### *4.2. Effects of Ca-Mg-B Foliar Application on Chlorophyll Content and Leaf Area Index in Korla Fragrant Pear*

Chlorophyll content (SPAD) and leaf area index (LAI) characterize the photosynthetic productivity potential of fruit trees from the perspectives of leaf photosynthetic pigment status and canopy structure, respectively. Together, they influence the interception of photosynthetically active radiation by the canopy and photosynthetic carbon assimilation capacity, and are closely associated with fruit tree growth and development and yield formation [31,32]. Magnesium (Mg) is the central atom of the chlorophyll molecule and is directly involved in the structural composition of the chlorophyll porphyrin ring; its content therefore directly affects the rate of chlorophyll synthesis and the functional integrity of the photosynthetic apparatus [33]. Calcium (Ca) maintains the stability of cell membranes and chloroplast membranes and protects the photosynthetic apparatus from oxidative damage, thereby contributing to the maintenance of high chlorophyll content and photosynthetic activity [34]. Boron (B) maintains cell-wall porosity and membrane integrity and promotes the transport of photosynthetic assimilates between source and sink organs, thereby indirectly affecting chlorophyll synthesis and photosynthetic efficiency [35]. In this study, SPAD

values exhibited a nonlinear response to increasing Ca–Mg–B application rates, initially increasing and subsequently declining. The highest SPAD value was observed under the M-CaMgB treatment, followed by a slight decrease under H-CaMgB; however, none of the differences among treatments reached statistical significance. These results indicate that, within the concentration range examined, combined foliar application of Ca–Mg–B exerted only a limited effect on leaf SPAD values in pear. Responses of leaf SPAD to foliar nutrient application have also been reported in sweet cherry [36] and apple [37]. The comparatively modest SPAD response observed in the present study may be attributable to the timing of application. Treatments were applied during the fruit enlargement stage, when leaves had already fully expanded and their chlorophyll-related physiological status was relatively stable, potentially limiting their responsiveness to additional foliar nutrient supply. In contrast to SPAD, LAI exhibited a more pronounced response to Ca–Mg–B concentration, following a similar rise-then-decline pattern and reaching its maximum under the M-CaMgB treatment. Comparable effects of nutrient supplementation on leaf area expansion and canopy development have been documented in apple [37,38], peach [39], and sweet cherry [36]. Moreover, Peng [40] reported that pear roots exhibit a certain degree of retention of Ca, Mg, and B, suggesting that foliar supplementation at specific developmental stages may provide a more rapid pathway for these nutrients to reach the leaves and exert their physiological effects.

LAI was significantly associated with eight mineral elements, with the strongest correlation observed for B ($r = 0.893$), indicating that LAI serves as an integrative indicator of overall mineral nutritional status: B promotes cell expansion and leaf extension through RG-II dimerization [41], whereas N and K drive cell division and canopy expansion [42]. In contrast, SPAD was significantly correlated only with N, Mn, Cu, and a few other elements, but not with Mg or Fe—despite the latter two being essential constituents of chlorophyll. This discrepancy can be attributed to the saturation effect of SPAD in the high-chlorophyll range [43,44] and further suggests that Mg and Fe supply was not limiting; rather, their uptake, dominated by Ca–Mg antagonism, proceeded asynchronously with that of other elements. From a practical perspective, the combined use of LAI and SPAD provides a rapid diagnostic tool for evaluating Ca-Mg-B regulation: the former reflects the overall status of multiple nutrients, whereas the latter is more sensitive to nitrogen. Moreover, the widespread positive correlations among mineral elements (e.g., N–Mn, Mn–B, and K–B) corroborate the coordinated uptake of macro- and micronutrients [45].

### *4.3. Effects of Ca-Mg-B Foliar Application on Physiological and Biochemical Responses in Korla Fragrant Pear*

In fruit trees, enhanced Rubisco activity indicates an increased capacity for photosynthetic carbon fixation and, consequently, a greater potential for assimilate supply to developing fruits, thereby providing an important material basis for yield formation. In the present study, Rubisco activity exhibited a clear "increase-then-decrease" response across the Ca-Mg-B concentration gradient, with the M treatment significantly increasing Rubisco activity by 2.71-fold compared with the control. Galerian et al. [46] directly demonstrated a significant stimulatory effect of Ca-B co-application on Rubisco activity, which is consistent with our finding that foliar application of Ca-Mg-B at an appropriate concentration markedly enhanced Rubisco activity. Notably, the H treatment resulted in a decline in Rubisco activity. The decline in Rubisco activity under the H-CaMgB treatment was consistent with the response reported by Bai et al. [47], who observed that the beneficial effects of foliar Mg application in grapevine diminished and shifted toward inhibition at higher application rates. A comparable pattern was reported by Lu et al. [39], who found that further increases in foliar Ca and Mg concentrations in peach conferred only limited additional benefits. Collectively, these findings suggest that Rubisco activity may exhibit a

concentration-dependent response to foliar Ca–Mg–B application, whereby appropriate application rates enhance carbon assimilation, whereas excessive application attenuates this stimulatory effect. This pattern further suggests the existence of an optimal application range for foliar Ca–Mg–B; however, the physiological and biochemical mechanisms underlying the decline in Rubisco activity at higher application rates remain to be clarified.

SOD, POD, and CAT constitute a major antioxidant enzyme system in plants. SOD catalyzes the dismutation of superoxide anions ($O_2^-$) into $H_2O_2$ and $O_2$, whereas POD and CAT further participate in $H_2O_2$ detoxification by converting it into $H_2O$ and $O_2$. Through their coordinated action, these enzymes form an integrated antioxidant defense chain that maintains cellular redox homeostasis and facilitates the effective scavenging of reactive oxygen species (ROS) [48]. In the present study, Ca-Mg-B treatments induced distinct enzyme-specific responses and exhibited a pronounced concentration-window effect. POD activity was significantly enhanced at the low concentration but subsequently declined with increasing micronutrient fertilizer concentration. In contrast, SOD and CAT activities displayed a clear "increase-then-decrease" pattern as Ca-Mg-B concentration increased, and the M treatment synergistically activated the SOD-CAT cascade. Wu et al. [49], in a sodium selenite concentration-gradient experiment on Dendrobium huoshanense, reported that POD activity reached its maximum under the low concentration of 0.3 mg $L^{-1}$, whereas SOD and CAT activities both initially increased and subsequently decreased, with significant enhancement observed at the intermediate concentrations of 0.3 and 3 mg $L^{-1}$. These results were also consistent with the findings of Zhao et al. [50]. The observation that the optimal induction concentration range for SOD and CAT was higher than that for POD may reflect functional differentiation and temporal coordination among different antioxidant enzymes within the ROS-scavenging network. Thus, the present results indicate that Ca-Mg-B application does not uniformly activate the antioxidant system, but rather induces enzyme-specific responses within distinct concentration windows.

PAL is a key and rate-limiting enzyme in the phenylpropanoid pathway, catalyzing the conversion of phenylalanine to cinnamic acid and initiating the biosynthesis of secondary metabolites such as flavonoids, lignin, and salicylic acid. Its activity is therefore closely associated with plant disease resistance [51]. PPO catalyzes the oxidation of phenolic compounds to quinones and participates in fruit browning and defense responses [52]. In the present study, PAL activity exhibited a distinct "increase-then-decrease" pattern, whereas PPO activity showed a wave-like fluctuation. Yan et al. [53] reported a pronounced concentration-window effect on PAL activity, while Kiani et al. [54] similarly observed considerable fluctuations in PPO activity. The M treatment enhanced PAL activity while suppressing PPO activity. Mekontso et al. [55] demonstrated that GABA treatment simultaneously increased PAL activity and effectively inhibited PPO activity, suggesting that coordinated "PAL upregulation-PPO suppression" may contribute to maintaining phenolic metabolic balance and preventing excessive oxidative damage. This pattern is consistent with our observation that PAL activity was significantly enhanced whereas PPO activity was significantly reduced under the M treatment. Malondialdehyde (MDA), a terminal product of membrane lipid peroxidation, is commonly used as an indicator of the extent of cellular membrane damage. Proline (PRO), in contrast, functions as an important osmotic-regulatory substance and antioxidant. Under stress conditions, PRO accumulation contributes to the maintenance of cellular osmotic balance, ROS scavenging, and protection of proteins and membrane structures. The present study revealed a progressive increase in PRO content alongside a gradual decline in MDA content across treatments; however, under the H-CaMgB treatment, PRO accumulation was further enhanced while SOD and CAT activities declined, suggesting that the PRO accumulation induced by Ca-Mg-B foliar application may carry a dual significance. On the one hand, moderate proline accumulation,

acting as an important osmoprotectant, can enhance plant adaptability to environmental fluctuations by maintaining cellular water balance, stabilizing membrane structures, and participating in ROS scavenging. On the other hand, excessive PRO accumulation may instead represent a defensive response triggered by the perception of ionic imbalance or latent stress. Particularly, enhanced antioxidant enzyme activities can effectively reduce ROS accumulation and membrane lipid peroxidation, consequently limiting MDA formation [56,57]. This mechanism is consistent with the observed increase in PRO accumulation and decrease in MDA content in the present study, suggesting that Ca-Mg-B treatment may alleviate oxidative stress in pear leaves by simultaneously enhancing osmotic adjustment and antioxidant defense capacity. Similarly, previous studies have cautioned that PRO accumulation alone cannot serve as a reliable indicator of enhanced stress tolerance, and that its interpretation requires comprehensive evaluation alongside antioxidant enzyme activities and oxidative damage markers [58]. Accordingly, the elevated PRO content coupled with the decline in SOD and CAT activities under the H treatment in the present study suggests that the H-CaMgB concentration exceeded the optimal regulatory range, thereby inducing mild ionic homeostatic stress. In contrast, the M treatment, by sustaining higher SOD and CAT activities together with lower MDA levels, proved more conducive to maintaining leaf redox homeostasis.

The widespread significant positive correlations between mineral elements and antioxidant/photosynthetic enzyme activities essentially reflect a direct correspondence between elemental chemical functions and enzyme molecular composition: Mn, Cu, and Zn serve as the active centers and structural components of Mn-SOD and Cu/Zn-SOD, respectively, whereas CAT is a heme–iron enzyme whose activity depends on the supply status of the corresponding ions [16]. As a constituent of enzymatic proteins and chlorophyll, N exhibited correlations as high as 0.88–0.91 with CAT and Rubisco, underscoring the role of nitrogen nutrition in sustaining enzyme protein synthesis. K, an activator of more than 60 enzymes, showed its strongest correlation with PAL ($r = 0.85$), indicating that potassium nutrition regulates phenylpropanoid metabolic flux [59], while $Mg^{2+}$ participates in carbon assimilation by activating Rubisco and stabilizing chlorophyll molecules [60]. Notably, PPO was significantly and negatively correlated only with B, which can be interpreted from two perspectives. On the one hand, B maintains the stability of cell walls and membrane systems through RG-II dimerization, such that adequate boron nutrition channels phenolic metabolism toward structural construction rather than oxidative consumption [61]. On the other hand, recent evidence suggests that PPO-mediated phenolic oxidation constitutes a metabolic overflow pathway that dissipates reducing power and perturbs cellular redox homeostasis under stress; its suppression thus reflects a decline in cellular oxidative stress [41]. The significant negative correlations of MDA with N and Mn are consistent with this logic: improved nitrogen and manganese supply strengthens the SOD–CAT cascade for reactive oxygen species scavenging, thereby alleviating membrane lipid peroxidation [62]. Finally, the significant negative correlation between PRO and Fe alone suggests that abnormal proline accumulation under excessive Ca-Mg-B application is accompanied by an imbalance in iron nutritional status, given that proline metabolism serves as a central hub through which plants integrate osmotic and oxidative stress signals [63].

### *4.4. Effects of Ca-Mg-B Foliar Application on Fruit Yield of Korla Fragrant Pear*

Calcium (Ca), magnesium (Mg), and boron (B) are essential mineral nutrients for fruit tree growth and development, and their coordinated nutritional balance plays an important role in yield formation. Ca and B exhibit synergistic interactions, with an adequate supply of B potentially promoting Ca uptake and translocation, while the complementary roles of Ca and Mg in maintaining cell membrane integrity may further contribute to

efficient nutrient acquisition. Therefore, the coordinated regulation of Ca, Mg, and B is of considerable importance for crop yield formation [64,65]. The present study revealed that both single fruit weight and yield exhibited a quadratic response to increasing Ca-Mg-B concentrations, initially rising and subsequently declining, with the M treatment eliciting the most pronounced enhancement of fruit enlargement and yield formation. Similarly, Haleema et al. [66], in a foliar Ca-B-Zn application experiment, reported that appropriate concentrations of Ca and B significantly enhanced yield and yield-related traits, whereas further increases in application concentration resulted in declines in some yield-related parameters, indicating a clear increasing-then-decreasing response to nutrient concentration. Álvarez-Herrera et al. [8] reported that the beneficial effects of B on fruit firmness and yield occurred within a distinct optimal concentration range, whereas further increases in B concentration reduced these effects. Likewise, Mostafapour et al. [67] demonstrated that B concentrations exceeding the optimal range could induce toxic effects, which is consistent with the response observed in the present study. Similarly, Galeriani et al. [46] suggested that the combined application of Ca and B could enhance yield by improving leaf photosynthetic efficiency, although the magnitude of this effect was dose dependent. Notably, yield-related physiological traits, including SPAD, LAI, Rubisco activity, SOD activity, CAT activity, and PAL activity, all exhibited their most favorable responses under the M treatment. This coordinated response indicates that the superior yield performance under the M treatment was associated with the simultaneous optimization of chlorophyll content (SPAD) and canopy structure (LAI), photosynthetic carbon assimilation (Rubisco), and antioxidant defense (SOD and CAT). Collectively, these coordinated physiological and biochemical responses may have contributed to the enhanced yield formation observed under the M treatment.

Meanwhile, the correlation network and Mantel test in this study indicate that the combined Ca-Mg-B application functions through a cascading pathway of "improving mineral nutrition—optimizing physiological traits—promoting yield formation," a coupling with a well-defined physiological basis: $Mg^{2+}$, as an essential cofactor of Rubisco and its activase, directly regulates photosynthetic carbon assimilation [68]; K participates in assimilate loading and fruit quality formation [69]; and Mn, Cu, and Zn constitute the active centers of antioxidant enzymes such as Mn-SOD and Cu/Zn-SOD, which accounts for the strongest Mantel coupling between mineral nutrition and physiological traits ($r = 0.85$). The high correlations of LAI, PAL, CAT, and Rubisco with yield ($r = 0.84$–$0.92$) demonstrate that the coordinated enhancement of canopy light interception, phenylpropanoid metabolism, reactive oxygen species scavenging, and carbon assimilation capacity constitutes the core of high-yield formation. Particularly noteworthy is that PPO was significantly negatively correlated with yield ($r = -0.653$) and highly significantly negatively correlated with B ($r = -0.74$). Recent evidence has confirmed that PPO disrupts photosynthetic electron transport and aggravates oxidative losses under plant stress responses [61], whereas B stabilizes cell walls and membrane systems through RG-II dimerization [41], suggesting that adequate boron nutrition may channel more carbon flux toward yield formation by suppressing PPO-mediated oxidative processes—offering a novel perspective that fertilization not only promotes synthesis but also reduces oxidative consumption. Furthermore, the continued Mg accumulation accompanied by a sharp PRO surge under the H treatment corroborates the classical assertion that proline metabolism acts as a hub in osmotic stress responses [63], underscoring the existence of a clear concentration threshold for foliar nutrition.

### *4.5. Limitations and Future Perspectives*

Although standardized washing with distilled water and sterile deionized water was performed prior to mineral element analysis, leaves were sampled only four days after the final foliar application; consequently, the possibility that residual fertilizer deposits influenced the measured Ca, Mg and B concentrations cannot be entirely excluded. The observed increases in leaf element contents should therefore be interpreted with caution. Future investigations would benefit from extending the sampling interval following foliar application or employing stable isotope tracing to disentangle the contributions of genuinely absorbed nutrients from those of surface residues. Furthermore, this study was conducted at a single orchard in over a single growing season; the generalizability of these findings thus warrants validation through multi-year field trials across diverse ecological environments.

## 5. Conclusions

The results of this study indicate that foliar application of Ca–Mg–B substantially influenced leaf mineral nutrition, physiological characteristics, and yield of Korla fragrant pear. Appropriate Ca–Mg–B application enhanced mineral nutrient uptake and improved the nutritional balance of the leaves, whereas excessive application reduced mineral nutrient uptake. Among all treatments, M-CaMgB, consisting of 0.2% Ca fertilizer, 0.4% Mg fertilizer, and 0.25% B fertilizer applied in combination, showed the best overall performance, yielding the highest values for leaf N, P, K, Ca, Mg, Mn, Cu, Zn, and B contents, SPAD, LAI, Rubisco activity, SOD activity, CAT activity, PAL activity, single-fruit weight, and yield. By contrast, the beneficial effects were less pronounced under the H-CaMgB treatment. Collectively, these findings suggest that, within the concentration range evaluated in this study, the moderate Ca–Mg–B treatment provided the most favorable overall response by maintaining a desirable leaf mineral nutritional status and physiological performance while promoting fruit yield. Accordingly, based on the preliminary findings obtained under the present experimental conditions, combined foliar application of 0.2% Ca fertilizer, 0.4% Mg fertilizer, and 0.25% B fertilizer during the fruit enlargement stage is recommended for 8- to 9-year-old Korla fragrant pear trees. Nevertheless, because these conclusions are derived from a single-year field experiment, their robustness and broader applicability should be further validated through multi-year and multi-location trials.

**Supplementary Materials:** The following supporting information can be downloaded at: https://www.mdpi.com/article/10.3390/horticulturae12111336/s1, Table S1: Partial least squares path model (PLS-SEM) specific indirect effects path coefficients; Table S2: Path coefficients and bootstrap confidence intervals of the partial least squares path model (PLS-SEM); Table S3: Outer loadings of the constructs with bootstrap statistics.

**Author Contributions:** Conceptualization, Y.K. and Z.C.; methodology, E.L.; formal analysis, X.G. and Y.K.; investigation, P.J. and K.W.; resources, E.L.; data curation, P.J., X.G., K.W. and E.L.; writing—original draft preparation, P.J.; writing—review and editing, Z.C.; visualization, Y.K.; supervision, Z.C.; project administration, Z.C.; funding acquisition, Z.C. All authors have read and agreed to the published version of the manuscript.

**Funding:** This research was funded by the Xinjiang Forest Fruit Industry Technology System—Soil Fertility and Cultivation (XJLGCYJSTX05-2024-03), and the National Natural Science Foundation of China (32360802, 31960639).

**Data Availability Statement:** The data presented in this study are available on request from the corresponding author due to the inclusion of unpublished Supplementary Experimental Data.

**Conflicts of Interest:** The authors declare no conflicts of interest.

## References


1. Marschner, H. *Mineral Nutrition of Higher Plants*, 2nd ed.; Academic Press: San Diego, CA, USA, 1995.
2. Cakmak, I.; Brown, P.; Colmenero-Flores, J.M.; Husted, S.; Kutman, B.Y.; Nikolic, M.; Rengel, Z.; Schmidt, S.B.; Zhao, F.-J. Chapter 7—Micronutrients This chapter is a revision of the third edition chapter by M. Broadley, P. Brown, I. Cakmak, Z. Rengel, and F.J. Zhao. In *Marschner's Mineral Nutrition of Plants*, 4th ed.; Rengel, Z., Cakmak, I., White, P.J., Eds.; Academic Press: San Diego, CA, USA, 2023; pp. 283–385.
3. Kutman, U.B. Chapter 9—Mineral nutrition and crop quality. In *Marschner's Mineral Nutrition of Plants*, 4th ed.; Rengel, Z., Cakmak, I., White, P.J., Eds.; Academic Press: San Diego, CA, USA, 2023; pp. 419–444.
4. Huang, W.; Shi, Y.; Yan, H.; Wang, H.; Wu, D.; Grierson, D.; Chen, K. The calcium-mediated homogalacturonan pectin complexation in cell walls contributes the firmness increase in loquat fruit during postharvest storage. *J. Adv. Res.* **2023**, *49*, 47–62. [CrossRef]
5. Ge, T.; Hanhan, Q.; Chunling, L.; Yue, X.; Ziquan, F.; Xinxiang, X.; Jingquan, L.; Mengxue, L.; Han, J.; Zhanling, Z.; et al. Magnesium improved fruit quality by regulating photosynthetic nitrogen use efficiency, carbon–nitrogen metabolism, and anthocyanin biosynthesis in 'Red Fuji' apple. *Front. Plant Sci.* **2023**, *14*, 1136179. [CrossRef]
6. O'Neill, M.A.; Eberhard, S.; Albersheim, P.; Darvill, A.G. Requirement of Borate Cross-Linking of Cell Wall Rhamnogalacturonan II for Arabidopsis Growth. *Science* **2001**, *294*, 846–849. [CrossRef]
7. Wei, D.; ZhiYong, P.; Bilal, H.S.; ZhongXing, H.; ShuAng, P.; YongZhong, L. Foliar Supplied Boron Can Be Transported to Roots as a Boron-Sucrose Complex via Phloem in Citrus Trees. *Front. Plant Sci.* **2020**, *11*, 250. [CrossRef]
8. Álvarez-Herrera, J.G.; Jaime-Guerrero, M.; Fischer, G. The Effect of Boron on Fruit Quality: A Review. *Horticulturae* **2025**, *11*, 992. [CrossRef]
9. Ullah, S.; Khan, A.S.; Malik, A.U.; Afzal, I.; Shahid, M.; Razzaq, K. Foliar Application of Boron Influences the Leaf Mineral Status, Vegetative and Reproductive Growth, Yield and Fruit Quality of 'Kinnow' Mandarin (*Citrus reticulata* Blanco.). *J. Plant Nutr.* **2012**, *35*, 2067–2079. [CrossRef]
10. Du, K.; Lin, H.; Luo, Q.; Li, T.; Wu, H.; Wang, B.; Guo, Z.; Pan, T.; She, W. Calcium and Boron Foliar Fertilizer to Relieve Cracking of 'Liuyuezao' Pummelos. *Foods* **2025**, *14*, 595. [CrossRef]
11. Khalaj, K.; Ahmadi, N.; Souri, M.K. Improvement of Postharvest Quality of Asian Pear Fruits by Foliar Application of Boron and Calcium. *Horticulturae* **2017**, *3*, 15. [CrossRef]
12. Alebidi, A.; Abdel-Sattar, M. Synergistic effect of seaweed extract and boric acid and/or calcium chloride on productivity and physico-chemical properties of Valencia orange. *PeerJ* **2024**, *12*, e17378. [CrossRef]
13. Guo, W.; Nazim, H.; Liang, Z.; Yang, D. Magnesium deficiency in plants: An urgent problem. *Crop J.* **2016**, *4*, 83–91. [CrossRef]
14. Chen, J.; Lü, J.; He, Z.; Zhang, F.; Zhang, S.; Zhang, H. Investigations into the production of volatile compounds in Korla fragrant pears (*Pyrus sinkiangensis* Yu). *Food Chem.* **2020**, *302*, 125337. [CrossRef]
15. Jiang, W.; Yan, P.; Zheng, Q.; Wang, Z.; Chen, Q.; Wang, Y. Changes in the Metabolome and Nutritional Quality of Pulp from Three Types of Korla Fragrant Pears with Different Appearances as Revealed by Widely Targeted Metabolomics. *Plants* **2023**, *12*, 3981. [CrossRef]
16. Lilay, G.H.; Thiébaut, N.; du Mee, D.; Assunção, A.G.L.; Schjoerring, J.K.; Husted, S.; Persson, D.P. Linking the key physiological functions of essential micronutrients to their deficiency symptoms in plants. *New Phytol.* **2024**, *242*, 881–902. [CrossRef]
17. Muneer, M.A.; Afridi, M.S.; Saddique, M.A.B.; Chen, X.; Zaib Un, N.; Yan, X.; Farooq, I.; Munir, M.Z.; Yang, W.; Ji, B.; et al. Nutrient stress signals: Elucidating morphological, physiological, and molecular responses of fruit trees to macronutrients deficiency and their management strategies. *Sci. Hortic.* **2024**, *329*, 112985. [CrossRef]
18. Liu, X.; Wang, Y.; Zhao, K.; Ke, Y.; Guo, Y.; Xue, Y.; Shen, X.; Chai, Z. Analysis of Soil Nutrient and Yield Differences in Korla Fragrant Pear Orchards Between the Core and Expansion Areas. *Agriculture* **2025**, *15*, 1873. [CrossRef]
19. Zhuang, Y.; Wang, X.; Gong, X.; Bao, J. Effects of Different Foliar Fertilizer Treatments on Fruit Quality of the Korla Fragrant Pear. *Horticulturae* **2024**, *10*, 51. [CrossRef]
20. Nelson, D.W.; Sommers, L.E. Determination of Total Nitrogen in Plant Material. *Agron. J.* **1973**, *65*, 109–112. [CrossRef]
21. Hansen, T.H.; Laursen, K.H.; Persson, D.P.; Pedas, P.; Husted, S.; Schjoerring, J.K. Micro-scaled high-throughput digestion of plant tissue samples for multi-elemental analysis. *Plant Methods* **2009**, *5*, 12. [CrossRef]
22. Lilley, R.M.; Walker, D.A. An improved spectrophotometric assay for ribulosebisphosphate carboxylase. *Biochim. Biophys. Acta (BBA)-Enzymol.* **1974**, *358*, 226–229. [CrossRef]
23. Abobatta, W.F.; El-Enin, M.M.S.A.; El-Zawily, H.M.A.E.-M.; Saif, M.I. Effect of foliar application of boric acid and ammonium molybdate on the productivity and fruit quality of Navel orange. *Sci. Hortic.* **2024**, *334*, 113290. [CrossRef]
24. Ahmed, N.; Zhang, B.; Chachar, Z.; Li, J.; Xiao, G.; Wang, Q.; Hayat, F.; Deng, L.; Narejo, M.-U.-N.; Bozdar, B.; et al. Micronutrients and their effects on Horticultural crop quality, productivity and sustainability. *Sci. Hortic.* **2024**, *323*, 112512. [CrossRef]
25. Vera-Maldonado, P.; Aquea, F.; Reyes-Díaz, M.; Cárcamo-Fincheira, P.; Soto-Cerda, B.; Nunes-Nesi, A.; Inostroza-Blancheteau, C. Role of boron and its interaction with other elements in plants. *Front. Plant Sci.* **2024**, *15*, 1332459. [CrossRef]

26. Al-Dulaimi, A.S.T.; Alrawi, D.S. Increasing the Absorption of Some Mineral Elements and the Quality of Apple Fruits by Foliar Spraying with Boron and Ascorbic Acid. *Migr. Lett*. **2023**, *20*, 365–374. [CrossRef]
27. Mutlag, L.; Mouhamad, R.; Al-Ghrairi, S. Effect of foliar fertilization in Coscia Pear seedlings on vegetative growth and biochemical characteristics. *DYSONA Appl. Sci*. **2020**, *1*, 51. [CrossRef]
28. Xie, K.; Cakmak, I.; Wang, S.; Zhang, F.; Guo, S. Synergistic and antagonistic interactions between potassium and magnesium in higher plants. *Crop J*. **2021**, *9*, 249–256. [CrossRef]
29. Vélez-Bermúdez, I.C.; Schmidt, W. Plant strategies to mine iron from alkaline substrates. *Plant Soil* **2023**, *483*, 1–25. [CrossRef]
30. Jarrell, W.M.; Beverly, R.B. The Dilution Effect in Plant Nutrition Studies. In *Advances in Agronomy*; Brady, N.C., Ed.; Academic Press: Cambridge, MA, USA, 1981; Volume 34, pp. 197–224.
31. Gitelson, A.; Viña, A.; Inoue, Y.; Arkebauer, T.; Schlemmer, M.; Schepers, J. Uncertainty in the evaluation of photosynthetic canopy traits using the green leaf area index. *Agric. For. Meteorol*. **2022**, *320*, 108955. [CrossRef]
32. Zhang, C.; Chen, Z.; Yang, G.; Xu, B.; Feng, H.; Chen, R.; Qi, N.; Zhang, W.; Zhao, D.; Cheng, J.; et al. Removal of canopy shadows improved retrieval accuracy of individual apple tree crowns LAI and chlorophyll content using UAV multispectral imagery and PROSAIL model. *Comput. Electron. Agric*. **2024**, *221*, 108959. [CrossRef]
33. Tränkner, M.; Tavakol, E.; Jákli, B. Functioning of potassium and magnesium in photosynthesis, photosynthate translocation and photoprotection. *Physiol. Plant*. **2018**, *163*, 414–431. [CrossRef]
34. Feng, D.; Wang, X.; Gao, J.; Zhang, C.; Liu, H.; Liu, P.; Sun, X. Exogenous calcium: Its mechanisms and research advances involved in plant stress tolerance. *Front. Plant Sci*. **2023**, *14*, 1143963. [CrossRef]
35. Blevins, D.G.; Lukaszewski, K.M. Boron in Plant Structure and Function. *Annu. Rev. Plant Biol*. **1998**, *49*, 481–500. [CrossRef]
36. Varaldo, A.; Giacalone, G. Enhancing Cracking Resistance and Post-Harvest Quality of Sweet Cherries (*Prunus avium* L.) Through Calcium and Potassium-Based Foliar Treatments. *Horticulturae* **2025**, *11*, 30. [CrossRef]
37. Wang, G.; Wang, J.; Han, X.; Chen, R.; Xue, X. Effects of Spraying Calcium Fertilizer on Photosynthesis, Mineral Content, Sugar–Acid Metabolism and Fruit Quality of Fuji Apples. *Agronomy* **2022**, *12*, 2563. [CrossRef]
38. Chauhan, P.; Sharma, N.C.; Sharma, D.P.; Kumar, P.; Chauhan, A. Combined effects of foliar nano-N and soil-applied N on growth, yield, and nutrient status in high-density apple orchards. *J. Plant Nutr.* **2026**, *49*, 2284–2314. [CrossRef]
39. Lu, C.; Wang, X.; Guo, X.; Hussain, B.; Wang, S.; Yang, X. Effects of Foliar Calcium and Magnesium Application on Peach (*Prunus persica* L.) Nutrition Status and Fruit Quality Formation. *Plants* **2026**, *15*, 2873. [CrossRef]
40. Peng, J.; Sun, Y.; Geng, J.; Xu, Z.; Wang, F.; Li, Z.; Wang, H.; Zhao, S. Comprehensive analysis of nutrient partitioning and microbial communities in pear orchards: Effects of tree age and spatial heterogeneity. *BMC Plant Biol*. **2025**, *25*, 1673. [CrossRef]
41. Hays, Q.; Lerouge, P.; Ropitaux, M.; Anderson, C.; Lehner, T. Storming the barricades of rhamnogalacturonan-II synthesis and function. *Plant Cell* **2025**, *37*, koaf088. [CrossRef]
42. Cao, W.; Sun, H.; Shao, C.; Wang, Y.; Zhu, J.; Long, H.; Geng, X.; Zhang, Y. Progress in the Study of Plant Nitrogen and Potassium Nutrition and Their Interaction Mechanisms. *Horticulturae* **2025**, *11*, 930. [CrossRef]
43. Padilla, F.M.; de Souza, R.; Peña-Fleitas, M.T.; Gallardo, M.; Giménez, C.; Thompson, R.B. Different Responses of Various Chlorophyll Meters to Increasing Nitrogen Supply in Sweet Pepper. *Front. Plant Sci*. **2018**, *9*, 1752. [CrossRef]
44. Xu, J.; Volk, T.A.; Quackenbush, L.J.; Stehman, S.V. Estimation of shrub willow leaf chlorophyll concentration across different growth stages using a hand-held chlorophyll meter to monitor plant health and production. *Biomass Bioenergy* **2021**, *150*, 106132. [CrossRef]
45. Fan, X.; Zhou, X.; Chen, H.; Tang, M.; Xie, X. Cross-Talks Between Macro- and Micronutrient Uptake and Signaling in Plants. *Front. Plant Sci*. **2021**, *12*, 663477. [CrossRef]
46. Galeriani, T.M.; Neves, G.O.; Santos Ferreira, J.H.; Oliveira, R.N.; Oliveira, S.L.; Calonego, J.C.; Crusciol, C.A.C. Calcium and Boron Fertilization Improves Soybean Photosynthetic Efficiency and Grain Yield. *Plants* **2022**, *11*, 2937. [CrossRef]
47. Bai, R.; Liu, H.; Liu, Y.; Yong, J.W.H. Effects of Foliar Application of Magnesium Fertilizer on Photosynthesis and Growth in Grapes. *Agronomy* **2024**, *14*, 2659. [CrossRef]
48. Apel, K.; Hirt, H. Reactive oxygen species: Metabolism, oxidative stress, and signal transduction. *Annu. Rev. Plant Biol*. **2004**, *55*, 373–399. [CrossRef]
49. Wu, Y.; An, C.; Wang, Y.; Sun, Y.; Liu, C.; Wang, B.; Qin, Y.; Zhang, Z. Dendrobium huoshanense In Vitro Culture and Selenium Metabolism: Speciation Mechanisms. *Horticulturae* **2025**, *11*, 1263. [CrossRef]
50. Zhao, Q.; Qin, M.; Lang, S.; Qin, M.; Liu, L.; Li, Q.; Zhang, D.; Li, L. Concentration-Dependent Effects of Foliar ZnO Nanoparticles on Growth and Nutrient Use in Young Crabapple Plants. *Horticulturae* **2025**, *11*, 1535. [CrossRef]
51. Zhu, B.; Zhang, Y.; Gao, R.; Wu, Z.; Zhang, W.; Zhang, C.; Zhang, P.; Ye, C.; Yao, L.; Jin, Y.; et al. Complete biosynthesis of salicylic acid from phenylalanine in plants. *Nature* **2025**, *645*, 218–227. [CrossRef]
52. Sui, X.; Meng, Z.; Dong, T.; Fan, X.; Wang, Q. Enzymatic browning and polyphenol oxidase control strategies. *Curr. Opin. Biotechnol*. **2023**, *81*, 102921. [CrossRef]

53. Yan, L.; Wang, M.; Yu, C.; Jia, P.; Gao, X.; Liu, E.; Chai, Z. Disease Resistance Response of Korla Fragrant Pear Branches to Potassium Fertilizer Application. *Horticulturae* **2026**, *12*, 532. [CrossRef]
54. Kiani, H.S.; Sabokdast, M.; Dedicova, B. Influence of Biotic and Abiotic Elicitors on Rosmarinic Acid Accumulation in Hairy Root Cultures of *Dracocephalum kotschyi* Boiss. *Plants* **2025**, *14*, 2809. [CrossRef]
55. Ngaffo Mekontso, F.; Duan, W.; Cisse, E.H.M.; Chen, T.; Xu, X. Alleviation of Postharvest Chilling Injury of Carambola Fruit by γ-aminobutyric Acid: Physiological, Biochemical, and Structural Characterization. *Front. Nutr.* **2021**, *8*, 752583. [CrossRef]
56. Ghorbani, A.; Pishkar, L.; Saravi, K.V.; Chen, M. Melatonin-mediated endogenous nitric oxide coordinately boosts stability through proline and nitrogen metabolism, antioxidant capacity, and Na+/K+ transporters in tomato under NaCl stress. *Front. Plant Sci.* **2023**, *14*, 1135943. [CrossRef]
57. Koc, Y.E.; Aycan, M.; Mitsui, T. Exogenous proline suppresses endogenous proline and proline-production genes but improves the salinity tolerance capacity of salt-sensitive rice by stimulating antioxidant mechanisms and photosynthesis. *Plant Physiol. Biochem.* **2024**, *214*, 108914. [CrossRef]
58. Spormann, S.; Nadais, P.; Sousa, F.; Pinto, M.; Martins, M.; Sousa, B.; Fidalgo, F.; Soares, C. Accumulation of Proline in Plants under Contaminated Soils—Are We on the Same Page? *Antioxidants* **2023**, *12*, 666. [CrossRef]
59. Ninkuu, V.; Aluko, O.O.; Yan, J.; Zeng, H.; Liu, G.; Zhao, J.; Li, H.; Chen, S.; Dakora, F.D. Phenylpropanoids metabolism: Recent insight into stress tolerance and plant development cues. *Front. Plant Sci.* **2025**, *16*, 1571825. [CrossRef]
60. Qin, H.; Zhang, X.; Tian, G.; Liu, C.; Xing, Y.; Feng, Z.; Lyu, M.; Liu, J.; Xu, X.; Zhu, Z.; et al. Magnesium alleviates growth inhibition under low potassium by enhancing photosynthesis and carbon-nitrogen metabolism in apple plants. *Plant Physiol. Biochem.* **2024**, *214*, 108875. [CrossRef]
61. Zou, H.; Xiao, Q.; Li, G.; Wei, X.; Tian, X.; Zhu, L.; Ma, F.; Li, M. Revisiting the advancements in plant polyphenol oxidases research. *Sci. Hortic.* **2025**, *341*, 113960. [CrossRef]
62. Pessoa, C.C.; Luís, I.C.; Daccak, D.F.; Legoinha, P.A.; Ramalho, J.C.; Lidon, F.C.; Silva, M.M. Mn's Key Roles in Plant Ecophysiology—A Comprehensive Review for Unstressed and Stress Conditions. *Agronomy* **2026**, *16*, 709. [CrossRef]
63. Renzetti, M.; Funck, D.; Trovato, M. Proline and ROS: A Unified Mechanism in Plant Development and Stress Response? *Plants* **2025**, *14*, 2. [CrossRef]
64. Singh, R.; Sharma, R.R.; Tyagi, S. Pre-harvest foliar application of calcium and boron influences physiological disorders, fruit yield and quality of strawberry (*Fragaria* × *ananassa* Duch.). *Sci. Hortic.* **2007**, *112*, 215–220. [CrossRef]
65. Engels, C.; Kirkby, E.; White, P. Chapter 5—Mineral Nutrition, Yield and Source–Sink Relationships. In *Marschner's Mineral Nutrition of Higher Plants*, 3rd ed.; Marschner, P., Ed.; Academic Press: San Diego, CA, USA, 2012; pp. 85–133.
66. Haleema, B.; Shah, S.T.; Basit, A.; Hikal, W.M.; Arif, M.; Khan, W.; Said-Al Ahl, H.A.H.; Fhatuwani, M. Comparative Effects of Calcium, Boron, and Zinc Inhibiting Physiological Disorders, Improving Yield and Quality of Solanum lycopersicum. *Biology* **2024**, *13*, 766. [CrossRef]
67. Mostafapour, F.; Amiri, J.; Jabbarzadeh, Z. Methyl jasmonate enhances boron toxicity tolerance in strawberry (*Fragaria* × *Ananassa* 'Albion') by modulating plant growth, antioxidant defenses, and biochemical responses. *BMC Plant Biol.* **2025**, *25*, 1453. [CrossRef]
68. Lobo, A.K.M.; Orr, D.J.; Carmo-Silva, E. Regulation of Rubisco activity by interaction with chloroplast metabolites. *Biochem. J.* **2024**, *481*, 1043–1056. [CrossRef]
69. Yang, H.; Xu, H.; Shi, Y.; Chen, L.; Zhang, L.; Kan, L.; Jin, Y.; Mei, X.; Xu, Y.; Ahmed, N.; et al. Molecular insights into the functional role of PbNRT2.4 in potassium homeostasis and nutrient transport in Pyrus ussuriensis. *Plant Stress* **2025**, *15*, 100752. [CrossRef]


**Disclaimer/Publisher's Note:** The statements, opinions and data contained in all publications are solely those of the individual author(s) and contributor(s) and not of MDPI and/or the editor(s). MDPI and/or the editor(s) disclaim responsibility for any injury to people or property resulting from any ideas, methods, instructions or products referred to in the content.